Siripong Malasri, **PhD, PE, CPLP Professional**
Editor-in-Chief, International Journal of Advanced Packaging Technology (ISSN 2349-6665)
Director, Healthcare Packaging Consortium, Christian Brothers University, 650 East Parkway South, Memphis, TN 38104, USA. Phone 1-901-321-3419; Fax 1-901-321-3402; Email pong@cloud-journals.com

Date: January 1, 2015

Dear Readers and Authors:

The **International Journal of Advanced Packaging Technology** is now entering its third year. In the previous two volumes most of the published articles were related to transport/distribution packaging. We would like to see articles in other areas of packaging, especially food packaging. In addition, we would like to see articles from more countries. You are invited to share your packaging expertise by submitting your work for possible publication in the journal.

If you have any comments/suggestions, please do not hesitate to let me know. We look forward to a more diverse Volume 3 in 2015. With your participation, the journal will be a great asset to the worldwide packaging community.

Sincerely,

S. Malasri

Siripong Malasri

Cloud Publications
International Journal of Advanced Packaging Technology
2015, Volume 3, Issue 1, pp. 138-146, Article ID Tech-341
ISSN 2349-6665, doi 10.23953/cloud.ijapt.18

Research Article | Open Access

Effect of Headspace Volume of Retort Pouches on Simulated Transport Hazards

Kyle Dunno, William Whiteside, Ron Thomas and Kay Cooksey

Department of Food, Nutrition, and Packaging Sciences, 223 Poole & Agricultural Center, Clemson University Clemson, SC, USA

Correspondence should be addressed to Kyle Dunno, kdunno@clemson.edu

Publication Date: 5 March 2015

DOI: https://doi.org/10.23953/cloud.ijapt.18

Abstract Institutional retort pouches containing either water or 5% starch solution were filled with varying amounts of headspace volume to determine if adding gaseous volume to the package can help it survive laboratory simulated engineering tests. Fixed displacement vibration testing and compression testing of the pouches yielded no differences in the amount of headspace volume. Significant differences were noted as a result of the shock testing (free fall drop method) when comparing the water filled pouches, but no headspace volume effect was observed for the 5% starch solution pouches. The results from this study showed increasing the headspace volume of a retort pouch does provide increased protection to transport hazards (shock) for a low viscosity food simulant as compared with a highly viscous product packaged similarly.
Keywords *Retort Pouch; Transport Hazards; Package Headspace*

1. Introduction

Institutional retort pouches are becoming more widely used as a replacement for the #10 can due to its ease of use and disposal [1]. Retort pouches help improve the safety for both consumers and employees. There are no sharp edges as there are with cans which eliminate cuts for both employees in the packaging plants and for the consumers opening the packages at home [2]. Due to retort pouches weighing significantly less than metal cans, they help lower transportation cost of moving the products throughout the supply chain. Pouches, empty and full, take up less storage space than comparable cans, jars, and trays [3]. Additionally, clear retort pouches, which were employed for this study, are becoming more widely used in applications where the ability to microwave, visibility of the product, and metal detection capabilities are of importance [4]. While all

of these features provide advantages to the product manufacturer and consumer, retort pouches do have disadvantages to the metal can such as slower filling speeds and lack of physical durability.

The effects of headspace volume and gas composition inside a retort pouch have been researched to understand the effects on thermal processing time and shelf life storage [5]. Previous research involving the physical durability of retort pouches has shown that pouch orientation and position has an effect on the performance and survival rate during vibration [6; 7]. These studies were conducted utilizing aluminum foil based retort pouches packaged in individual paperboard cartons.

Over-the-road truck transportation, rail transportation, and aircraft transportation are common channels packages pass through. Through these distribution channels packages are subjected to three major categories of dynamic hazards: shock, vibration, and compression [8]. Another hazard having an adverse effect on package performance is the environmental conditions at which it is transported and stored. A packages ability to withstand these hazards is vital to ensuring the products arrive safe and in usable condition.

The objective of this research was to understand how headspace volume affects the performance of individual retort pouches during laboratory simulated hazards. Product viscosity and storage temperatures were varied and evaluated to determine their effects on the pouches ability to resist critical failures resulting in loss of product. The performance of the pouches through these simulations can determine how it will survive through physical transportation.

2. Materials and Methods

The institutional pouch chosen for this experiment was a 1.5 kg four sided seal retort pouch constructed of aluminum oxide (AlOx) coated polyethylene terephthalate (PET)/biaxially oriented nylon (BON)/cast polypropylene (CPP) (Cryovac® Sealed Air, Duncan, SC). The retort pouches were filled with two food simulants: water and 5% starch solution. The water represented products having a low viscosity, while the 5% starch solution represented a more viscous product.

The headspace volume varied from 0 cubic centimeters (cc) to 400cc in 100cc intervals. This was done for both the water and 5% starch solution pouches. In order to calculate headspace volume, the sealed pouch was submerged in water with a graduated cylinder. The pouch was opened and the pouch was slowly compressed into the opening of the graduated cylinder. The displaced volume inside the graduated cylinder was recorded. Figure 1 provides an illustration on how the headspace volume was captured and recorded [9]. Five samples from each simulant and headspace volume were randomly selected and the average overall gas content was determined for that variable.

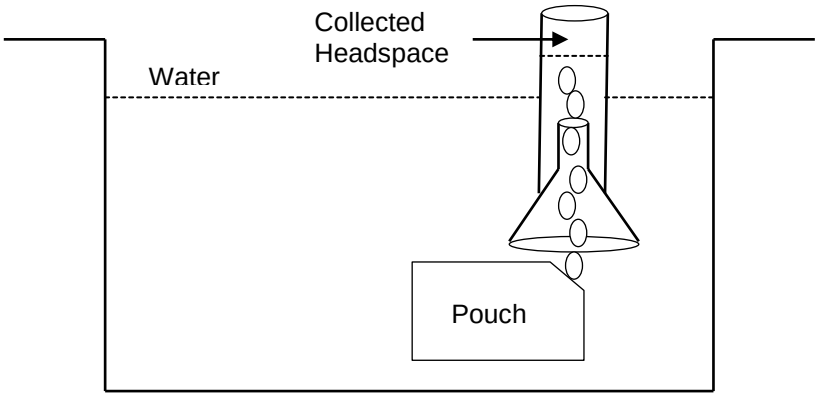

Figure 1: *Illustration for Headspace Volume Recording*

Storage conditions of the individual pouches also varied. The pouches were either stored at 23°C and 50% RH (standard conditions) or at 5°C and 85% RH (refrigerated conditions) per ASTM D4332 [10]. The pouches were held under these conditions for 24 hours prior to testing. Prior to filling the retort pouches a seal analysis was performed on the pouch to determine the optimal seal temperature for the pouches. The seals were evaluated using a SATEC Universal Tester and following ASTM F88 [10]. The heat seal temperature selected was 350°F with a dwell time of 2.5 seconds. Figure 2 illustrates the seal curves of both the pre- and post-retort pouches.

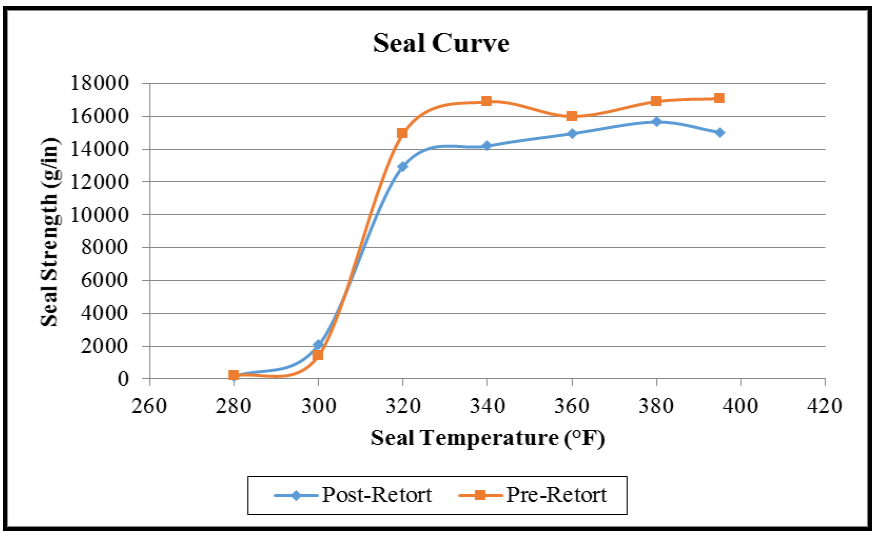

Figure 2: *Heat Seal Curve for Retort Pouch*

The retort pouches were filled using a Furakawa/Old Rivers FF-300NU pouch-sealing machine. The heat seal temperature was 350°F with a dwell time of 2.5 seconds. The average filled pouch weight of the water pouches was 1.38 ± 0.10 kg. The average filled pouch weight of the 5% starch solution pouches was 1.36 ± 0.11 kg.

A pilot scale rotary retort was employed for this experiment. The filled pouches were processed for 30 minutes at 250°F (after come-up) and 30 psi using a Surdry Model APR-95 Rotary Pilot Retort (Stock America, Cary, North Carolina). After being processed the viscosity of the two simulants was calculated by using a Brookfield Viscometer. The viscosity of the water was 1 cps and the viscosity of the 5% starch solution was 39,000 cps.

Upon conditioning, single pouches were subjected to individual laboratory simulated engineering tests, which included vibration, compression, and shock. Table 1 displays the number of samples used for each of the engineering tests. Only critical failures were reported during this research. A critical failure was determined to be a pouch failure that resulted in a visible loss of product.

Table 1: *Test Protocol Setup and Sample Size*

Headspace Volume (cc)	Vibration (Sample Size)		Compression (Sample Size)		Shock (Sample Size)	
	Standard	Refrigerated	Standard	Refrigerated	Standard	Refrigerated
0	5	5	20	20	20	20
100 ± 5	5	5	20	20	20	20
200 ± 5	5	5	20	20	20	20
300 ± 5	5	5	20	20	20	20
400 ± 5	5	5	20	20	20	20

2.1. Vibration

Sinusoidal vibration was used to evaluate pouch performance during vibration. Individual pouches were oriented such that the largest surface area was in contact with the vibration table. A Lansmont Vibration Tester Model 1500 was used to perform all vibration tests. ASTM D999 Method A1 (Repetitive Shock Test) was used to perform this experiment [10]. In order to keep refrigerated conditions for those pouches during the vibration test, large insulated coolers were attached directly to vibration table and instrumented with TH10 (Extech® Instruments, Nashua, New Hampshire) temperature data loggers to ensure conditions were maintained.

The test parameters used to drive the vibration table to create enough energy to cause the pouches to oscillate were set to 4.3 Hz and 0.96 G. Test parameters defined by using a 1/16 in. shim that would intermittently pass underneath the pouches. The pouches were vibrated for 60 minutes.

2.2. Compression

Compression testing of the pouches was performed referencing ASTM D642 [10]. An Interlaken Compression Tester (Interlaken Technology, Chaska, MN) was used to compress the individual pouches. Pouches were compressed using a fixed upper platen at a rate of 0.5 in/min. The pouches were compressed to failure recording peak force in pounds (lbs.) and deflection in inches (in.). Twenty pouches from each variable were compressed and the average and standard deviation were calculated for both the maximum force required for critical failure and the corresponding deflection at critical failure.

2.3. Shock

A free fall drop method was used for shock evaluation of the product. Individual pouches were impacted on the face of the pouch with the largest surface area. A Lansmont PDT 56 Drop Tester was used to perform all drop tests. The drop test procedure utilized to perform this experiment was ASTM D5276 [10]. The progressive drop test protocol within the ASTM D5276 standard to determine the critical drop height for each variable being analyzed. The initial drop height for each variable was 48 inches, and the drop height was increased in intervals of 4 inches until critical failure to pouch or a drop height of 72 inches was recorded.

2.4. Statistical Analysis

Data were analyzed as one-way ANOVAs using the generalized linear model procedure of SAS (version 9.1; SAS Institute, Cary, NC). When significant differences ($P \leq 0.05$) occurred among the treatments, the least significant difference test at $P = 0.05$ was used to separate the means.

3. Results and Discussion

3.1. Vibration

At the conclusion of each vibration test cycle, the pouches were visually inspected for critical failures (Table 2). It was determined that for all of the samples evaluated, no critical failures had been recorded. Critical failures were not observed as a result of the vibration due to the lack of force generated on the pouch seals. Although the product simulants were oscillating on the vibration table, there was not enough force exerted onto the pouch seals to create a critical failure. Because no pouch failures occurred, no statistical comparisons could be made on how headspace volume and product viscosity affect the pouches performance during vibration. Based on these results, it was determined vibration alone was not a critical distribution hazard for individual pouches.

Table 2: *Vibration Phase Results*

Headspace Volume (cc)	Standard Conditions		Refrigerated Conditions	
	Test Samples	Number of Failures	Test Samples	Number of Failures
0	5	0	5	0
100 ± 5	5	0	5	0
200 ± 5	5	0	5	0
300 ± 5	5	0	5	0
400 ± 5	5	0	5	0

3.2. Compression

The compression results displayed in Figures 3 and 4 illustrate the average maximum force required to create a critical failure. Statistical analysis was performed independently on the data sets comparing storage temperature and force required for pouch failure on both the water and 5% starch solution using ANOVA. It was concluded that for both the water and the 5% starch solution data sets there was a difference between the mean maximum force required for pouch failure at $P<0.05$. One general trend observed in both of these figures is the refrigerated pouches had a lower compressive force when compared to the standard pouches of the same headspace volume. This is due to the CPP having a glass transition temperature (Tg) near the refrigeration storage conditions resulting in the seals becoming more brittle at lower temperatures causing the seals to fail at a lower force [11].

The deflection results displayed in Figures 5 and 6 illustrate the maximum deflection required to create a critical failure at the corresponding maximum force. Statistical analysis was performed independently on the data sets for both the water and 5% starch solution using ANOVA. For both the water and the 5% starch solution data sets there was not a statistical difference between the means at $P=0.05$.

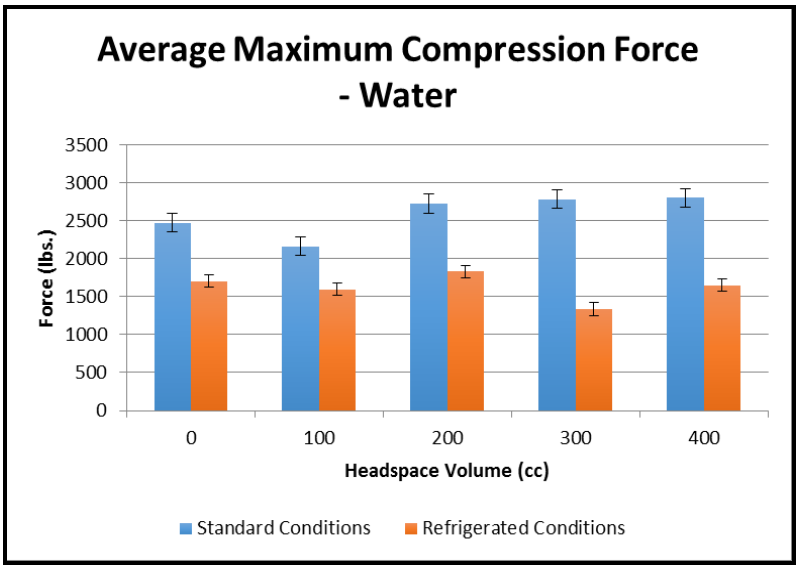

Figure 3: *Average Maximum Compression Force for Pouches Filled With Water*

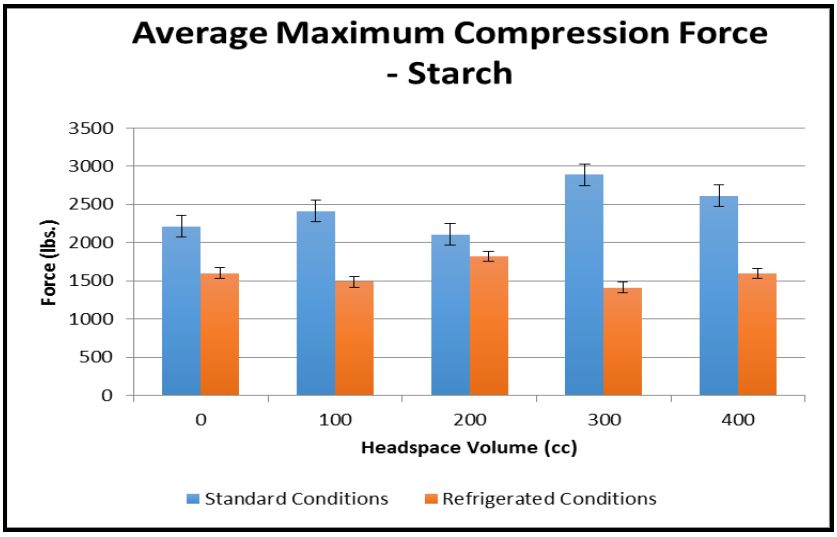

Figure 4: *Average Maximum Compression Force for Pouches Filled With 5% Starch Solution*

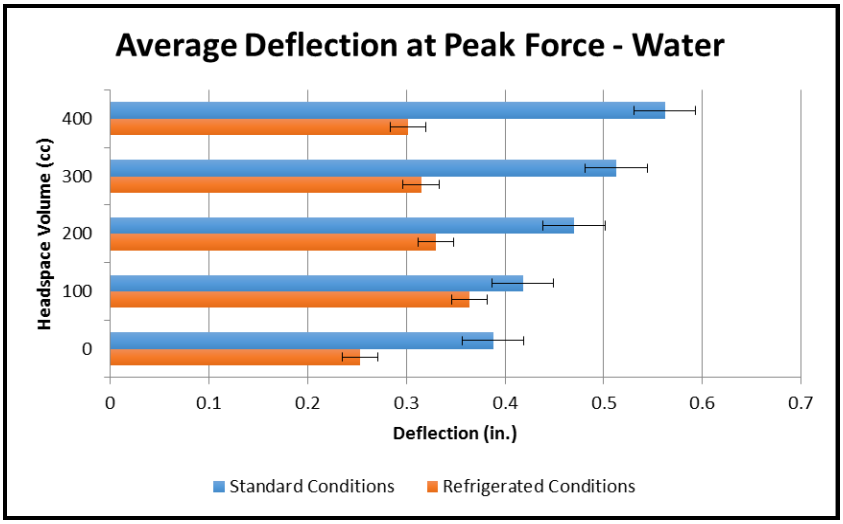

Figure 5: *Average Peak Deflection at Critical Failure for Pouches Filled With Water*

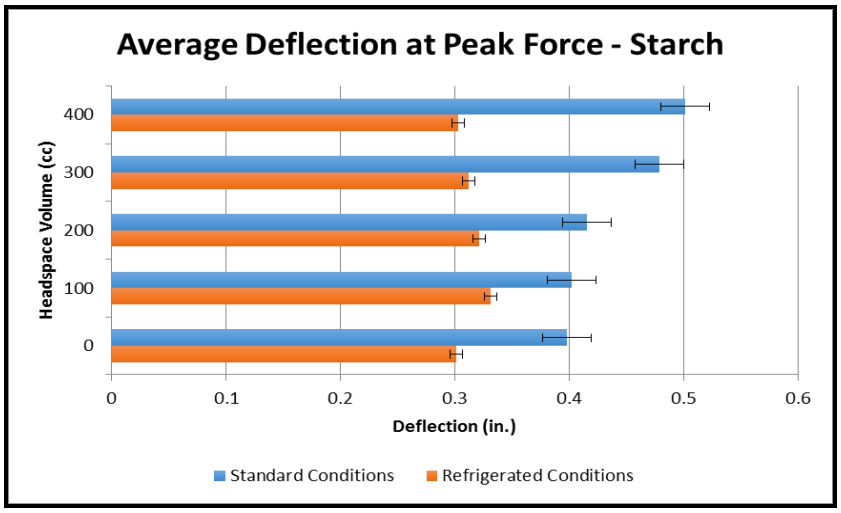

Figure 6: *Average Peak Deflection at Critical Failure for Pouches Filled With 5% Starch Solution*

3.3. Shock

The critical drop heights displayed in Figure 7 show averaged drop height required for a critical failure of the pouches filled with water. A similar trend, noted previously during the compression phase, shows again the refrigerated pouches generally had a lower critical drop height than when compared to the standard pouches. An ANOVA was performed on the data set for the water filled pouches and it was concluded at $P<0.05$ there was a difference between the mean critical drop height and pouch headspace volume. Further analysis was conducted comparing the mean drop heights of the standard and refrigerated pouches to the headspace volume. Statistical differences between headspace volumes of 0cc and 100cc were reported, but there was no statistical difference between headspace volumes of 200cc, 300cc, and 400cc at $P=0.05$ when comparing the mean drop height of the standard to the refrigerated pouches. Analysis of the refrigerated pouches shows there was a difference in the mean critical drop height and pouch headspace volume ($P<0.05$). This trend shows for the refrigerated retort pouches filled with water, the increased headspace volume inside the pouch resulted in a greater critical drop height prior to critical failure. The increased headspace volume inside the retort pouch appears to act as a cushion or shock absorber for the refrigerated pouches allowing them to be dropped from greater heights before failure.

Figure 8 displays the averaged critical drop heights required for a critical pouch failure for the pouches filled with 5% starch solution. An ANOVA was performed on the data set for the 5% starch solution filled pouches and at $P<0.05$ there was not a statistical difference between the means. When comparing the two product simulants, the headspace volume has less affect on pouch performance with the 5% starch solution (more viscous product) than it does with the water filled pouches. The pouches filled with the starch solution were more viscous and had different dynamic properties compared to the water filled pouches. Because of this, the force to the seals on the retort pouches was not as great with the starch filled pouches as they were with the water filled pouches. For the water filled pouches the headspace volume appears to aid in cushioning the pouches during the drop whereas this is not required for a more viscous product.

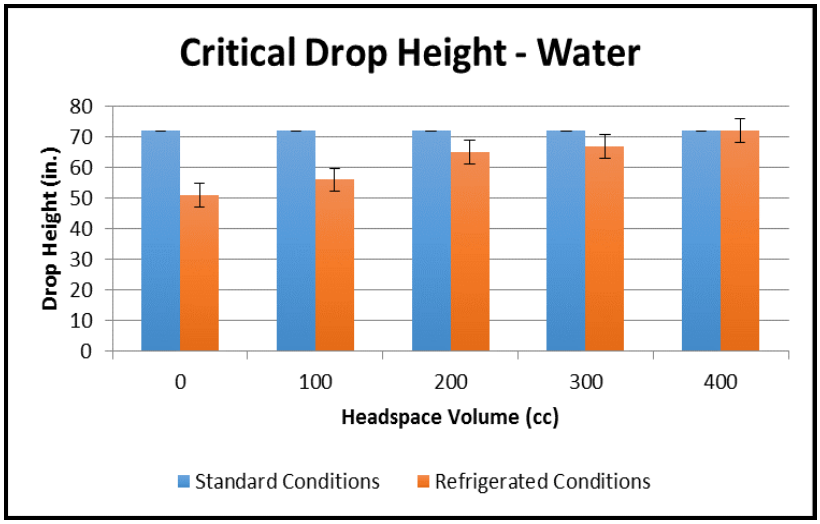

Figure 7: *Comparison of Critical Drop Height – Water Filled Pouches*

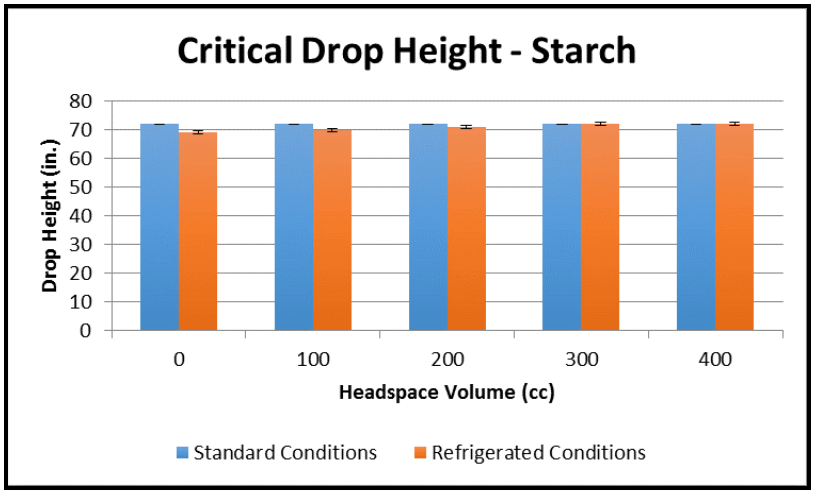

Figure 8: *Comparison of Critical Drop Height – 5% Starch Solution Filled Pouches*

4. Conclusions

This research study examined the effects of individual laboratory simulated transport hazards on retort pouches filled with different food simulants while varying the headspace volume. These pouches were then processed and stored in either standard or refrigerated conditions prior to being evaluated by laboratory simulated engineering tests. It was determined sinusoidal vibration was not a critical distribution hazard to the retort pouch. Both simulants along with the varied storage conditions recorded no critical failures, and no statistical difference was determined for the headspace volume.

Compression of the individual pouches yielded results showing statistical differences between the storage conditions, but no statistical differences between the headspace volume ($P<0.05$). This was a result of the CPP becoming brittle at the refrigerated conditions. The pouches with greater headspace volume could be deflected more before the pouch seal ruptured, but this was due to the headspace volume being able to be compressed.

Shock testing produced results showing that headspace volume did have an effect on pouch performance, especially at the refrigerated storage conditions. For pouches stored at refrigerated conditions the greater the headspace volume the higher drop height the pouch could withstand. Analysis shows there was not a statistical difference between the drop height and headspace volume for the 5% starch solution pouches, but there was for the water filled pouches ($P<0.05$). The shock test concluded headspace volume has a greater affect on pouch performance for lower viscosity food products than for more highly viscous products.

This research explored headspace volume, product viscosity, and storage temperature and how each affects a retort pouch during laboratory simulated hazards. Although retort pouches are shelf stable and do not require refrigeration, pouches could be exposed to extreme temperatures during transportation throughout the supply chain from manufacturer to consumer. The research shows increasing the headspace volume inside a retort pouch could increase the pouches ability to arrive safely to the consumer, especially in cold temperatures.

References

[1] Brooks, D.E. *The Retort Pouch–Practical Considerations in Its Use*. Retrieved 05 Jul 13 from: http://www.aseanfood.info/Articles/13001934.pdf.

[2] Mykytiuk, A., 2002: *Retort Flexible Packaging: The Revolution Has Begun.* Flexible Packaging. 18-25.

[3] Al-Baali, A.G. and Farid, M.M., 2006: *Sterilization of Food in Retort* Pouches. New York: Springer Science + Business Media, LLC.

[4] Whiteside, S.W., 2005: *Introduction to Retort Pouch Technology*. TAPPI PLACE Conference. Las Vegas, NV.

[5] Sepulveda, D., Olivas, G., Rodriguez, J., Warner, H., Clark, S. and Barbosa-Canovas, G. *Storage of Retort Pouch Beefsteak and Beef Stew Under Four Headspace Levels.* Journal of Food Processing Preservation. 2003. 27 (3) 227-242.

[6] Kongcharoenkiat, P., 1980: *Simulated Transit Vibration Damage on Retort Pouches*. M.S. Thesis, Michigan State University.

[7] Rukspollamuang, N., 1983: *Physical Damage and the Effect of Vibration on the Oxygen Barrier Quality of Institutional Retort Pouches*. M.S. Thesis, Michigan State University.

[8] Brandenburg, Richard and Lee Julian June-Ling, 2001: *Fundamentals of Packaging Dynamics*. L.A.B. Equipment, Inc.

[9] Ugaz, J., 2010: *Retardation of Browning and Softening of Thermally Processed Pears Packed in Retortable Pouches*. M.S. Thesis, Rutgers. The State University of New Jersey.

[10] ASTM International, 2012: *Selected ASTM Standards on Packaging*. Philadelphia, PA.

[11] Biron, M., 2007: *Thermoplastics and Thermoplastic Composites: Technical Information for Plastics Users*. Oxford, UK: Butterworth-Heinemann.

Cloud Publications
International Journal of Advanced Packaging Technology
2015, Volume 3, Issue 1, pp. 129-137, Article ID Tech-348
ISSN 2349-6665, doi 10.23953/cloud.ijapt.17

Research Article **Open Access**

Experimental Verification of McKee Formula

Badar Aloumi, Waleed Alnashwan, Siripong Malasri, Alex Othmani, Michael Kist, Nathan Sampson, Sebastian Polania, Yuliana Sanchez-Luna, Matthew Johnson and Ronald Fotso

Healthcare Packaging Consortium, Christian Brothers University, 650 East Parkway South, Memphis, TN, USA

Correspondence should be addressed to Siripong Malasri, pong@cbu.edu

Publication Date: 13 February 2015

DOI: https://doi.org/10.23953/cloud.ijapt.17

Abstract Seventy RSC single-wall 200# corrugated boxes, of seven different sizes from the same manufacturer, were compressed. Actual box compression strengths were compared with those computed using the McKee formula. The ratios of side-loading to top-loading box compression strengths for 3”x3”x3”, 5”x5”x5”, and 7”x7”x7” were found to be 30%, 46%, and 62% below those derived from the formula, while the box compression strengths (top loading) were 18%, 45%, and 63% higher. Bigger boxes yielded wider discrepancy between the actual compression strength value and that predicted by the McKee formula. A similar conclusion was made with three other box sizes with the same height (4”x4”x12”, 5”x5”x12”, and 6”x6”x12”). The effect of box height (which is not included in McKee formula) on its compression strength was also investigated using three box sizes, 5”x5”x5”, 5”x5”x12”, and 5”x5”x48”. As expected, the box became weaker as the height increased due to the wall buckling. The compression strength dropped 62% from the 5” to 48” box heights. Overall, the box compression strengths (BCT) predicted by the McKee formula were off anywhere from 50.48% overestimate for the 5”x5”x48” box size to 69.36% underestimate for the 6”x6”x12” box size.

Keywords *McKee Formula; Box Compression Strength; Corrugated Boxes; Edge Compression Test (ECT)*

1. Introduction

Corrugated boxes are the most commonly used secondary packaging for shipping goods. The McKee formula has been widely used to predict the compression strength of corrugate boxes. The formula is defined as [1]:

$$BCT = 5.876 \times ECT \times \sqrt{U \times d} \qquad \text{..... Equation 1}$$

where *BCT* = Box compression test/strength (lb), *ECT* = Edge crush test (lb/in), *U* = Footprint perimeter (in), and d = Wall thickness (in).

In this study, a verification of McKee formula compression strength was done experimentally by crushing a total of 70 RSC (regular slotted container) single-wall 200# corrugated boxes of seven different sizes from the same manufacturer. The effects of loading direction, footprint perimeter, volume, and height on the boxes' compression strength were investigated.

2. Materials and Methods

The following RSC box sizes were used in this study: 3"x3"x3", 4"x4"x12", 5"x5"x5", 5"x5"x12", 5"x5"x48", 6"x6"x12", and 7"x7"x7". They were grouped for various studies, as shown in Table 1. Eighteen measurements of wall thickness were made from various boxes (Table 2). Edge crush tests were performed on 2"x2" specimens cut from various boxes using the Clamp Method in accordance to TAPPI T839 [2], as shown in Table 2 and Figure 1. Specimen orientations for top and side loadings are shown in Figure 2.

Table 1: *Box Grouping for Various Studies*

Group	Box Size	Study
1	3"x3"x3", 5"x5"x5", 7"x7"x7"	• Effect of Load Direction • Effect of Footprint Perimeter (Cube Shape) • Effect of Volume (Cube Shape)
2	4"x4"x12", 5"x5"x12", 6"x6"x12"	• Effect of Footprint Perimeter (Same Height) • Effect of Volume (Same Height)
3	5"x5"x5", 5"x5"x12", 5"x5"x48"	• Effect of Height

Table 2: *Wall Thickness & ECT*

No.	Wall Thickness (in)
1	0.112
2	0.124
3	0.104
4	0.101
5	0.090
6	0.100
7	0.102
8	0.095
9	0.114
10	0.115
11	0.128
12	0.094
13	0.108
14	0.109
15	0.088
16	0.110
17	0.115
18	0.126
Avg (in)	*0.108*
SD (in)	*0.012*
SD (% of Avg)	*11.02*

No.	ECT (lb)	
	Top Load	Side Load
1	63.94	35.43
2	76.91	40.44
3	71.61	38.94
4	74.03	33.39
5	61.56	37.89
6	67.69	37.48
7	59.72	45.82
8	53.67	36.31
9	60.88	37.81
10	62.39	32.39
11	52.52	34.51
12	50.21	31.93
13	62.06	36.77
14	47.62	37.48
15	48.39	32.05
16	56.8	38.69
17	47.91	38.73
18	59.55	33.26
Avg (lb)	*59.86*	*36.63*
SD (lb)	*8.88*	*3.48*
SD (% of Avg)	*14.84*	*9.51*
Side/Top	*0.61*	
ECT (lb/in)	*29.93*	*18.31*

Figure 1: *ECT Using Clamp Method Per TAPPI T839*

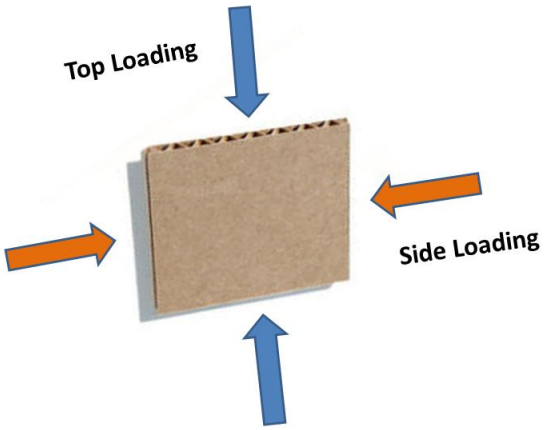

Figure 2: *ECT Specimen Orientations for Top and Side Loadings*

Boxes were crushed on a compression table and maximum/failure loads were recorded, as shown in Figure 3 and Table 3.

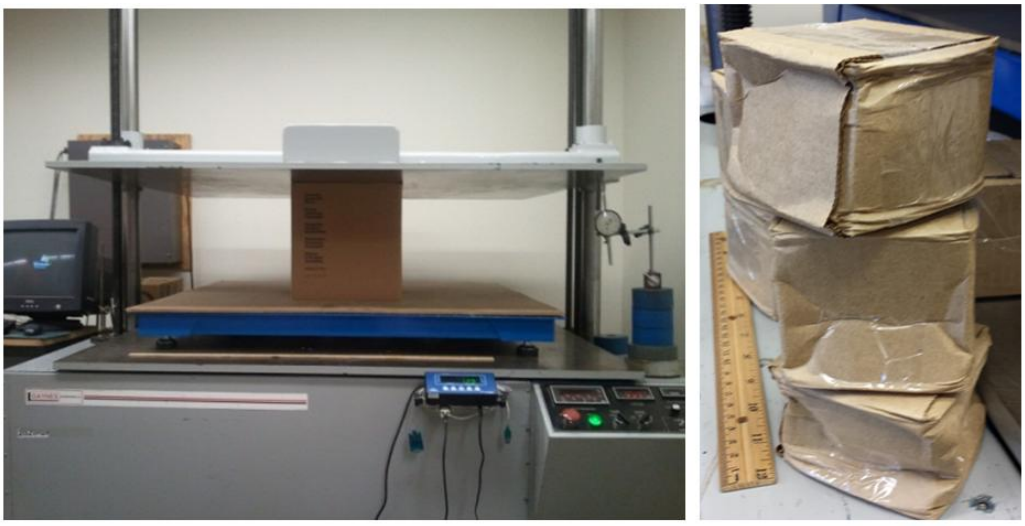

Figure 3: *Compression Test of Boxes*

Table 3: *Compression Test Data*

LxWxH	3"X3"X3"	5"X5"X5"	4"X4"X12"	5"X5"X12	7"X7"X7"	6"X6"X12"	5"X5"X48"
Height, H (in)	3	5	12	12	7	12	48
Footprint Perimeter, U (in)	*12*	*20*	*16*	*20*	*28*	*24*	*20*
Volume (in^3)	*27*	*125*	*192*	*300*	*343*	*432*	*1200*
No.	**Box Compression Strength, Top Load (lb)**						
1	262	326	304	317	509	460	139
2	293	394	316	286	521	482	120
3	268	352	313	313	522	487	139
4	263	331	291	316	504	500	118
5	242	342	274	327	528	461	106
6	269	332	279	305	533	441	137
7	224	327	298	289	491	506	132
8	218	350	293	301	517	479	128
9	236	342	278	308	518	477	141
10	241	311	304	325	485	491	117
Avg (lb)	*252*	*341*	*295*	*309*	*513*	*478*	*128*
SD (lb)	*23*	*22*	*15*	*14*	*16*	*20*	*12*
SD (% of Avg)	*9.24*	*6.57*	*4.98*	*4.48*	*3.03*	*4.13*	*9.32*

3. Results and Discussion

3.1. Effect of Load Direction

Three box sizes (3”x3”x3”, 5”x5”x5”, and 7”x7”x7”) were used. For each size, 10 boxes were crushed by top loading and another 10 boxes by side loading. ECT of 29.93 and 18.31 lb/in from Table 2 were used in BCT calculations from the McKee formula (Equation 1) for top and side loadings, respectively. Results were summarized in Table 4 and Figure 4. Side/Top BCT ratio was constant at 0.61, which was the Side/Top ECT ratio. However, when the trend line equation of actual compression data in Figure 4 was used, Side/Top ratios from the experiment were 0.43 for U = 12” (3”x3”x3” box size) and 0.23 for U = 28” (7”x7”x7” box size), respectively. This represents 30% and 62% below the 0.61 ratio obtained from the McKee formula.

Table 4: *Effect of Load Direction*

	Top & Side Max Load (lb), 200# Single Wall					
	3"x3"x3"		5"x5"x5"		7"x7"x7"	
No.	**Top Load**	**Side Load**	**Top Load**	**Side Load**	**Top Load**	**Side Load**
1	262	118	326	106	509	126
2	293	95	394	112	521	139
3	268	116	352	105	522	132
4	263	106	331	108	504	134
5	242	103	342	103	528	130
6	269	114	332	107	533	119
7	224	98	327	111	491	128
8	218	118	350	120	517	107
9	236	108	342	104	518	114
10	241	112	311	98	485	103
Avg	*252*	*109*	*341*	*107*	*513*	*123*
SD	*23*	*8*	*22*	*6*	*16*	*12*
SD (% of Avg)	*9.24*	*7.55*	*6.57*	*5.56*	*3.03*	*9.73*
BCT (lb)	*200*	*122*	*258*	*158*	*305*	*187*
U (in)	***12***		***20***		***28***	
Side/Top (Actual)	***0.43***		***0.32***		***0.24***	
Side/Top (BCT)	***0.61***		***0.61***		***0.61***	

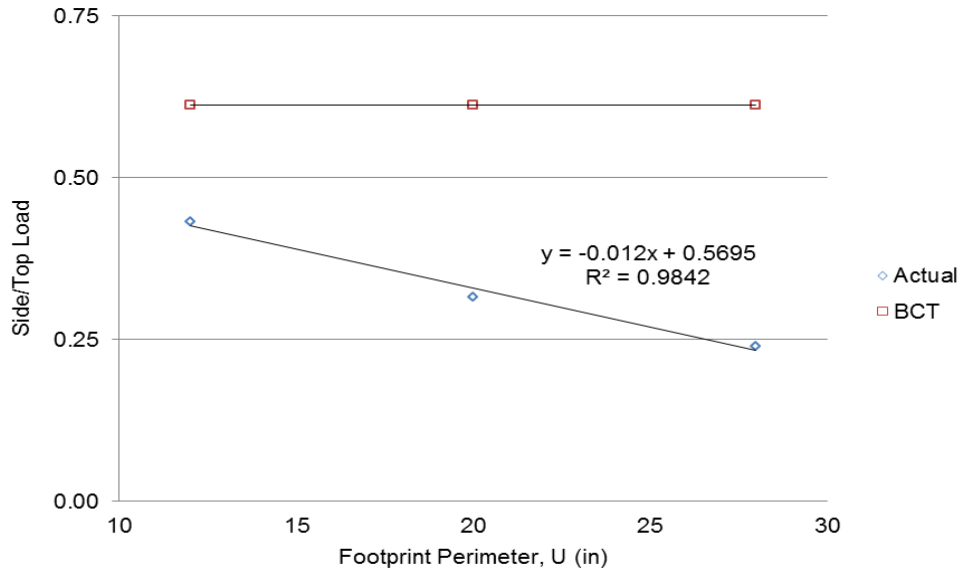

Figure 4: *Side/Top Load Ratio versus Footprint Perimeter*

3.2. Effect of Footprint Perimeter and Volume

In this experiment, two sets of boxes were used. The first set consisted of three cube boxes; 3”x3”x3”, 5”x5”x5”, and 7”x7”x7”. The data for this set was presented in Table 4 and only top-load data was used in this analysis. The second set consisted of three box sizes with the same height of 12”; 4”x4”x12”, 5”x5”x12”, and 6”x6”x12”. Results were summarized in Table 5 and Figures 5 and 6. Using trend line equations from Figure 5, the box strengths from experiment were 18% and 63% over those obtained from the McKee formula (BCT) for U = 12” (3”x3”x3” box size) and U = 28” (7”x7”x7” box size), respectively. Similarly, trend line equations from Figure 6 yielded 16% and 60% over BCT for U = 16” (4”x4”x12” box size) and U = 24” (6”x6”x12” box size), respectively.

Table 5: *Effect of Footprint Perimeter and Volume*

No.	Box Compression Strength (lb)					
	Same Box Proportion, Cube			Same Box Height, 12"		
	3"x3"x3"	5"x5"x5"	7"x7"x7"	4"x4"x12"	5"x5"x12"	6"x6"x12"
1	262	326	509	304	317	460
2	293	394	521	316	286	482
3	268	352	522	313	313	487
4	263	331	504	291	316	500
5	242	342	528	274	327	461
6	269	332	533	279	305	441
7	224	327	491	298	289	506
8	218	350	517	293	301	479
9	236	342	518	278	308	477
10	241	311	485	304	325	491
Avg (lb)	***252***	***341***	***513***	***295***	***309***	***478***
SD (lb)	*23*	*22*	*16*	*15*	*14*	*20*
SD (% of Avg)	*9.24*	*6.57*	*3.03*	*4.98*	*4.48*	*4.13*
BCT (lb)	***200***	***258***	***305***	***231***	***258***	***282***
U (in)	***12***	***20***	***28***	***16***	***20***	***24***
Volume (in^3)	***27***	***125***	***343***	***192***	***300***	***432***

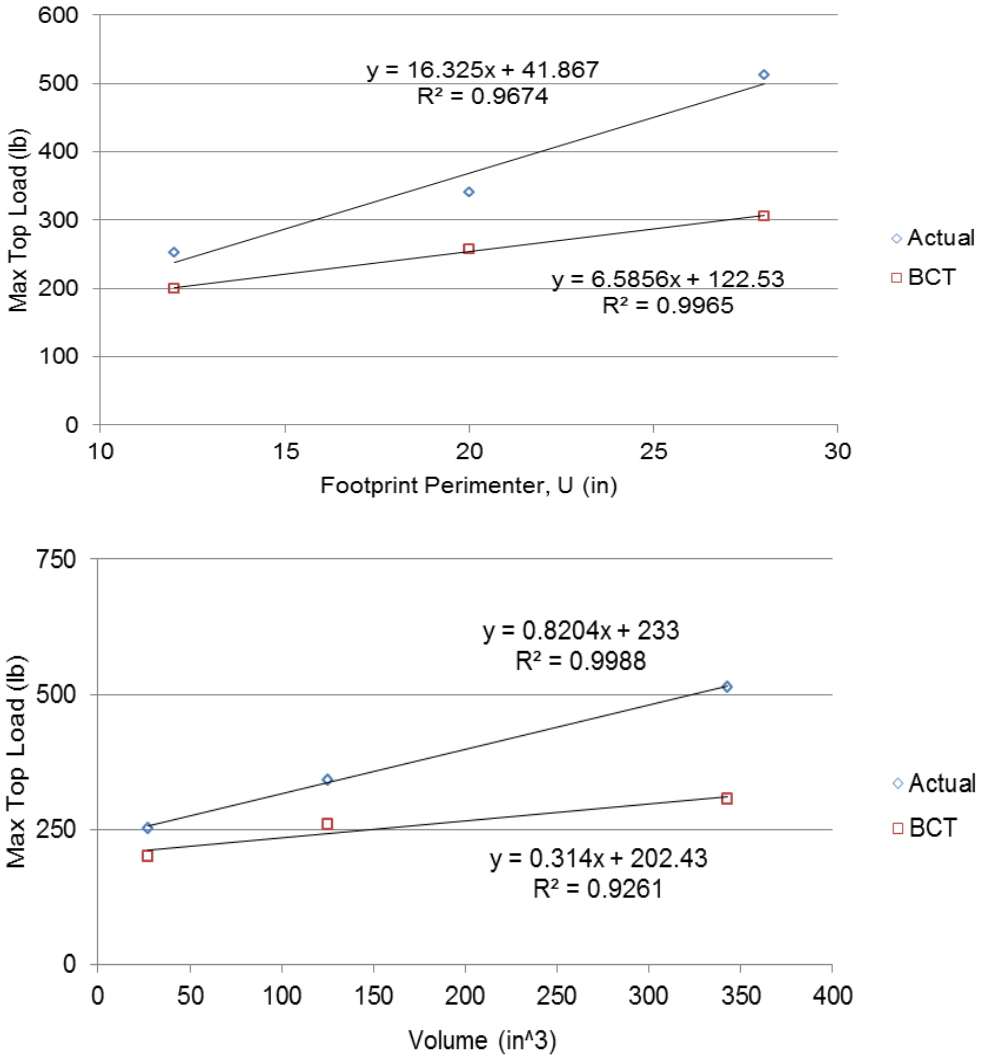

Figure 5: *Effect of Footprint Perimeter and Volume – Cube Boxes*

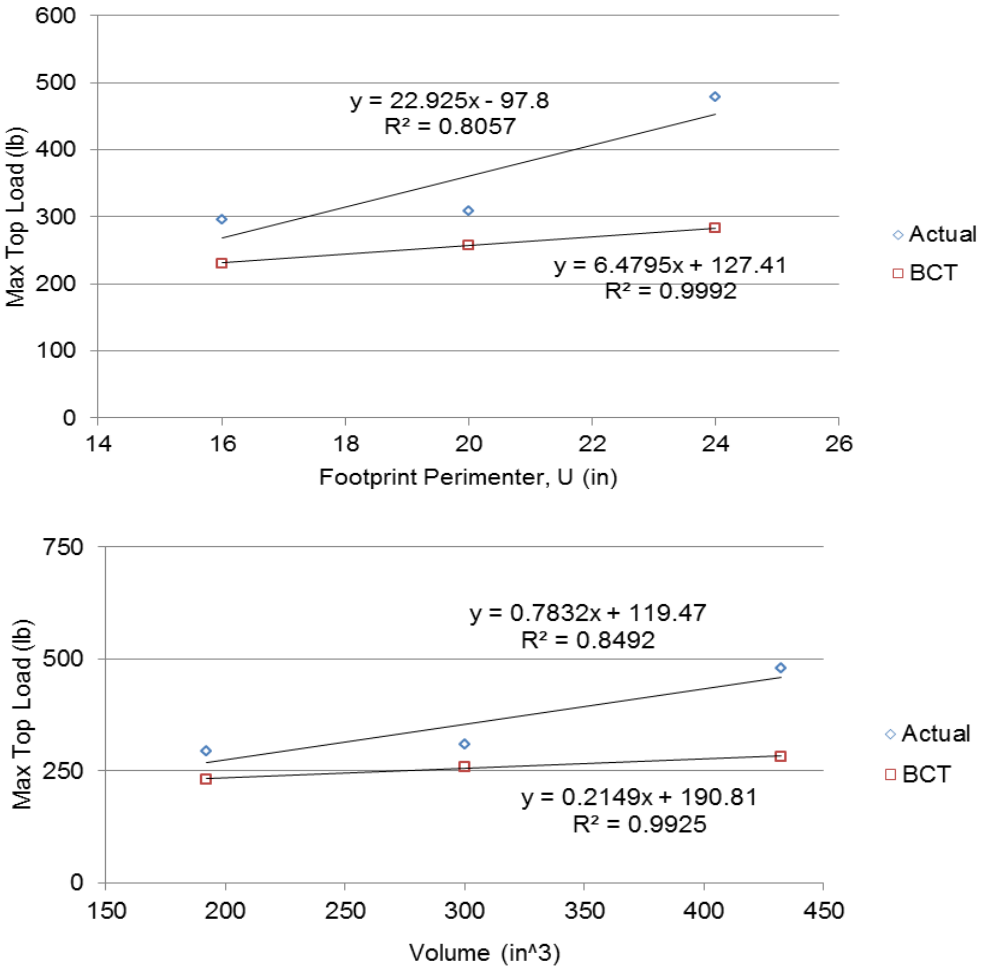

Figure 6: *Effect of Footprint Perimeter and Volume – Boxes with Same Height*

Using the trend line equations from Figure 5, the box strengths from the experiment were 21% and 66% greater those predicted from the McKee formula (BCT) for Volume = 27 in^3 (3”x3”x3” box size) and Volume = 343 in^3 (7”x7”x7” box size), respectively. Similarly, the trend line equations from Figure 6 yielded 16% and 61% greater BCT for Volume = 192 in^3 (4”x4”x12” box size) and Volume = 432 in^3 (6”x6”x12” box size), respectively.

3.3. Effect of Height

Three box sizes were used in this experiment. Each box size had the same footprint of 5”x5” but varied in height of 5”, 12”, and 48”. Ten boxes of each size were crushed, and the data was summarized in Table 6. Results were plotted in Figure 7. Using the trend line equations from Figure 7, the box strengths from experiment were 33% over and 51% under those obtained from the McKee formula (BCT) for Height = 5 in (5”x5”x5” box size) and Height = 48 in (5”x5”x48” box size), respectively.

Table 6: *Effect of Height*

No.	Box Compression Strength (lb)		
	5"x5"x5"	5"x5"x12"	5"x5"x48"
1	326	317	139
2	394	286	120
3	352	313	139
4	331	316	118
5	342	327	106
6	332	305	137
7	327	289	132
8	350	301	128
9	342	308	141
10	311	325	117
Avg (lb)	***341***	***309***	***128***
SD (lb)	*22*	*14*	*12*
SD (% of Avg)	*6.57*	*4.48*	*9.32*
BCT (lb)	***258***	***258***	***258***
Height (in)	***5***	***12***	***48***

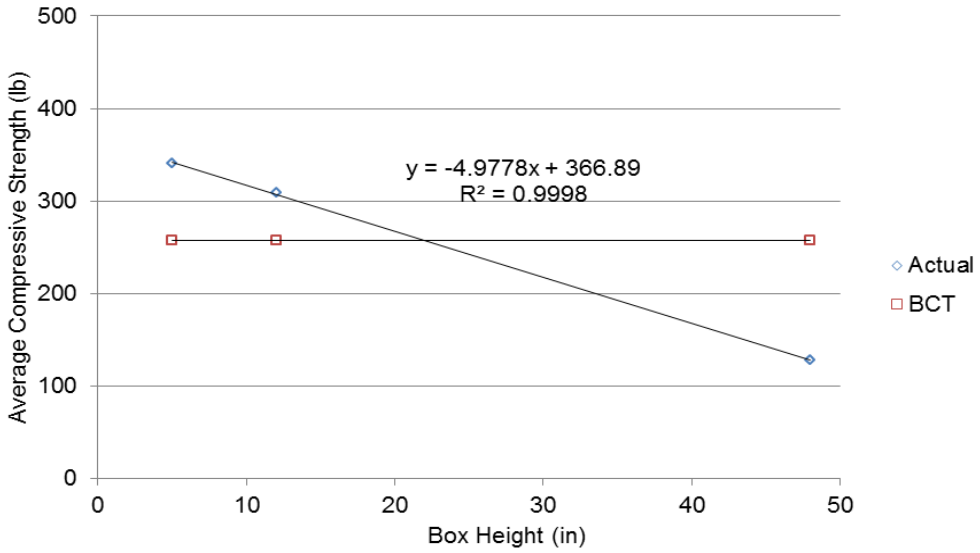

Figure 7: *Effect of Height*

3.4. Box Compression Strength

Further analysis of data is summarized in Table 7 and Figure 8.

Table 7: *Box Strengths*

	3"X3"X3"	5"X5"X5"	4"X4"X12"	5"X5"X12	7"X7"X7"	6"X6"X12"	5"X5"X48"
Actual Strength (lb)	*252*	*341*	*295*	*309*	*513*	*478*	*128*
McKee Strength, BCT (lb)	*200*	*258*	*231*	*258*	*305*	*282*	*258*
% Diff from BCT	*25.96*	*32.12*	*27.90*	*19.71*	***68.07***	*69.36*	***-50.48***
Volume (in^3)	*27*	*125*	*192*	*300*	*343*	*432*	*1200*
Strength/in of Volume (lb/in^3)	*9.32*	*2.73*	*1.54*	*1.03*	*1.50*	*1.11*	*0.11*

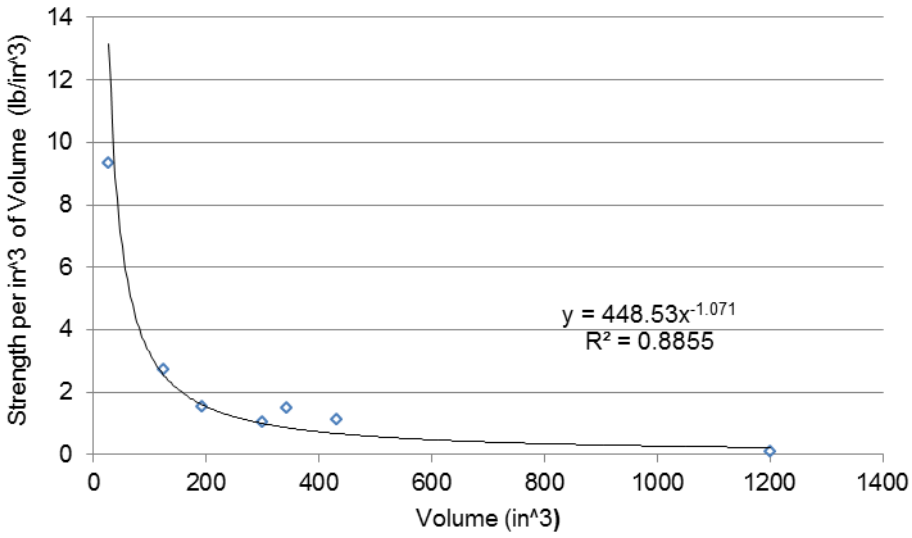

Figure 8: *Box Strength per Unit Volume*

4. Conclusion

The experimental data, obtained from seventy RSC single-wall boxes in seven sizes, showed that the box compression strengths (BCT) predicted by the McKee formula were off anywhere from 50.48% overestimate for the 5”x5”x48” box size to 69.36% underestimate for the 6”x6”x12” box size (Table 7). As the box volume increases, its compression strength per unit volume decreases rapidly as can be seen in Figure 8.

Only seven box sizes were included in this study. This represents only a small fraction of corrugated boxes commonly used. The results of this study must be used with caution. More data would be needed to improve these results. For example, it is well known that a buckling curve is not linear unlike the trend line shown in Figure 7. However, the goal of this study was to verify the accuracy of the McKee formula. Results from this study, using various angles of examination, indicate that the McKee formula could be off significantly.

Acknowledgement

Part of the data was presented at the 2014 HPC Fall Meeting (November 2014). Use with permission from Christian Brothers University.

References

[1] Wikipedia, 2014: *Edge Crush Test*. http://en.wikipedia.org/wiki/Edge_crush_test.

[2] TAPPI, 2008: *TAPPI T839: Edgewise Compressive Strength of Corrugated Fiberboard Using the Clamp Method (Short Column Test).*

Cloud Publications
International Journal of Advanced Packaging Technology
2015, Volume 3, Issue 1, pp. 147-157, Article ID Tech-412
ISSN 2349-6665, doi 10.23953/cloud.ijapt.19

Research Article **Open Access**

Effect of Temperature on Drinking Water Bottles

Siripong Malasri, Ali Pourhashemi, Robert Moats, Antoine Herve, Joseph Ferris, Asit Ray, and Ray Brown

Healthcare Packaging Consortium, Christian Brothers University, 650 East Parkway South, Memphis, TN, USA

Correspondence should be addressed to Siripong Malasri, pong@cbu.edu

Publication Date: 18 May 2015

DOI: https://doi.org/10.23953/cloud.ijapt.19

Abstract Two drinking water bottle sizes; 10 Fl. Oz. and 16.9 Fl. Oz., were crushed across a range of temperatures, from $32^{\circ}F$ to $125^{\circ}F$. Three sets of bottles were placed in a temperature chamber at $150^{\circ}F$, in refrigerator, and in freezer for about three hours. Another set of bottles were kept at room temperature. Bottle compression strength reduced at a rate of about 0.5 and 0.3 pound per 1 $^{\circ}F$ increase in temperature for the 10 and 16.9 Fl. Oz. respectively. Bulging was observed at the bottom of the 16.9 Fl. Oz. bottles. It was stabilized at about 5 hours under $150^{\circ}F$. However, leaks occurred shortly after the temperature was elevated to $170^{\circ}F$. In addition, the strength per bottle of a 24-bottle pack was found to be about 25% more than that of single bottle strength.
Keywords *Drinking Water Bottles; High Temperature; Bulging*

1. Introduction

Bottled water has been widely consumed due to convenience and cleanliness. In 2008, bottled water sales accounted for about 8.6 billion U.S. gallons, which was about 29% of the U.S. beverage market [1]. Bottle manufacturers have reduced the materials used through thickness reduction and clever structural design of water bottles. During distribution and transport, bottled water is often placed in a high temperature environment.

In a previous study [2], the temperature inside a truck container could easily reach $150^{\circ}F$ during a hot summer day based on the following heat transfer equation (Equation 1):

$$T_i - T_\infty = \left(\frac{q_s \alpha}{1.91/W^{1/4} + 2.84H^{3/4}\left(\frac{1}{W} + \frac{1}{L}\right)} \right)^{0.8} \quad \text{..... Equation 1}$$

Where T_i = interior temperature of tractor trailer (°C), T_∞ = exterior temperature (°C), q_s = sun load (1000 W/m^2), α = absorptivity of solar radiation, L = length of tractor trailer (m), H = height (m), and W = width (m). As the temperature rose, it was found that wooden pallet compression resistance weakened.

This article reports the effect of high temperatures on the compression strength and bulging of bottled water.

2. Materials and Methods

2.1. Polyethylene Terephthalate (PET)

Most of the beverage bottles, used in the USA, are manufactured using PET (polyethylene Terephthalate) and PET modified by copolymerization by the use of added co-monomer. PET is relatively strong, withstands higher temperature (has high melting point), and has good barrier properties against moisture, oxygen, CO_2, alcohol, and solvents. It can be made transparent by limiting crystallinity using copolymerization, adding fillers or controlling cooling when melt-processed during manufacture. PET bottles made for containing water are amorphous (non-crystalline) or have low crystallinity for clarity and toughness. However, one of the disadvantages of PET is its low melt strength which makes it difficult or impossible to process to make bottles by the standard extrusion blow molding. Melt strength can be improved by copolymerization using any number of co-monomers or increasing molecular weight during polymerization, i.e. when making polymer resins [3].

Hence, water bottles sold by different vendors are expected to be made from PET's having minor differences in chemical constituents - in terms of types and quantities of co-monomers added during polymerization and molecular weight (intrinsic viscosity) attained during the process. Because of this fact, the percentage of crystallinity and tendency for crystallization can vary from one set of bottles to another; hence, their responses to temperature, humidity, compressions, drops, shocks, and vibrations experienced during transportation/distribution can vary significantly. A significant factor in the growth of PET containers, in the market, is the high value and performance characteristics that it maintains even after being recycled. It has the highest recycling rate of all plastics.

The properties of PET polymer include: density of 1.33-1.38 gm/cm^3 (amorphous), transparency of 85-92%, melting point of 255-260°C, tensile strength of 58 MPa, tensile elongation of 150-300%, and processing temperature of 275-295°C [4]. Additional properties can be found on Wikipedia [5].

2.2. Chamber Dwell Time

Two bottle sizes commonly found in grocery stores were used in this study: 10 Fl. Oz. and 16.9 Fl. Oz. However, only the larger size was used in the bulging experiment. Sets of bottles were placed in a freezer, refrigerator, environmental chamber (set at 150 $^\circ F$), and at room temperature. The dwell time in the freezer, refrigerator, and environmental chamber was about three hours, which was more than the minimum dwell time determined from a simplified form of the Fourier equation of cylindrical

coordinate unsteady state heat conduction, as shown in Equation 2 [6] and backed up with experimental data:

$$t := \frac{r^2}{5.78\alpha} \ln\left[0.692 \frac{T_s - T_o}{T_s - T_f}\right] \quad \text{..... Equation 2}$$

Where t = time for water to reach equilibrium (minutes), r = liquid radius, α = thermal diffusivity = $\frac{k}{\rho C_p}$, T_s = surface temperature ($^\circ F$), T_o = initial temperature of water ($^\circ F$), T_f = final average temperature of water ($^\circ F$), k = thermal conductivity as shown in Figure 1, ρ = water density (62.4 lb/ft^3), and C_p = water heat capacity (1 BTU/lb$^\circ F$).

Based on Equation 2, the time for water to reach 95% of a chamber temperature between 80$^\circ F$ to 180$^\circ F$ was in the range of 42.6 to 48.9 minutes for T_s. This was backed up by an experiment where thermocouples were used to measure water temperature (T_f) and surface temperature (T_s) in a 16.9 Fl. Oz. bottle, as shown in Figure 2. It took about 100 minutes for the water temperature (T_f) to reach 150$^\circ F$. Thus, the 3-hour chamber dwell time at 150$^\circ F$ used in this study was more than sufficient.

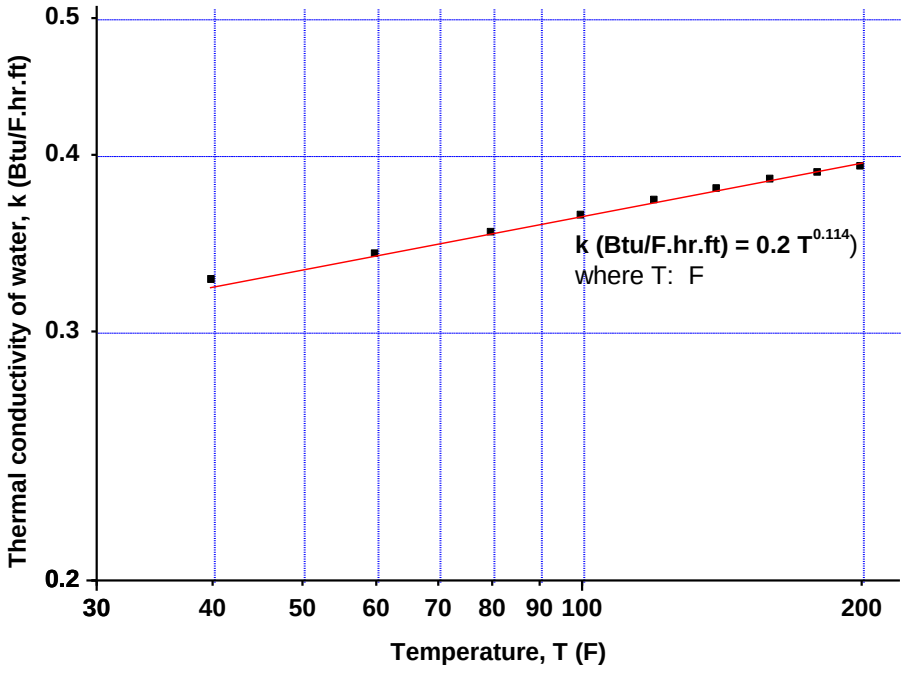

Figure 1: *Thermal Conductivity of Water as a Function of Temperature*

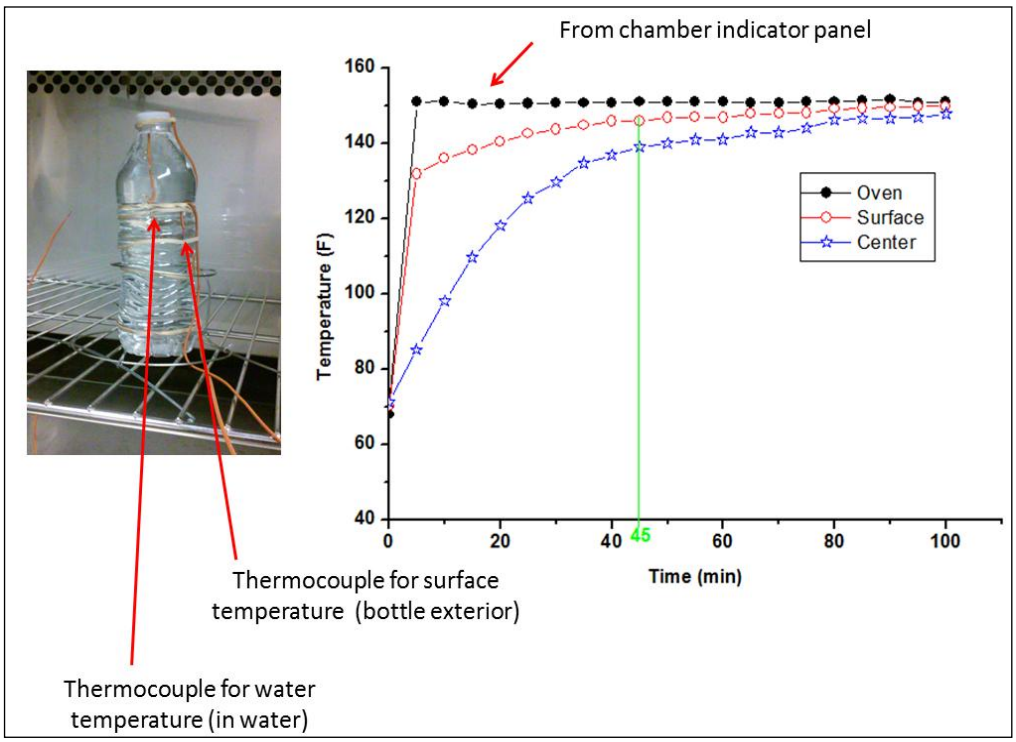

Figure 2: *Heating of Water Bottle*

2.3. Compression Test and Surface Temperature Measurement

Bottles were taken from the chamber, refrigerator, and freezer to a compression table, along with those dwelled in room temperature. A hand-held thermocouple reader was used to determine the bottle exterior temperature at the time of the compression test (Figure 3). Force was applied at the rate of 0.5 inch/minute.

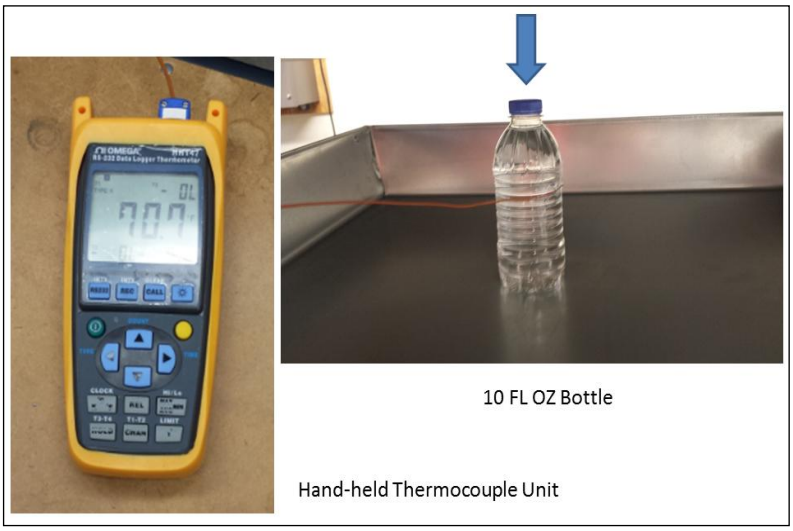

Figure 3: *Measuring Bottle Temperature at the Time of Compression Test*

The bulging at the bottom of the 16.9 Fl. Oz. bottles was much more pronounced than in the 10 Fl. Oz. bottles. Thus, it was difficult to make a bulged bottle stand vertically while being compressed. Thus, a simple supporting fixture was designed to ensure the verticalness of the bottle, as shown in Figure 4. The foam at the bottom of a corrugated box prevented the slippage while the brush on the top held the bottle vertically with a minimum of lateral force due to the flexibility of the brush hairs. Compression test data was summarized in Tables 1 and 2.

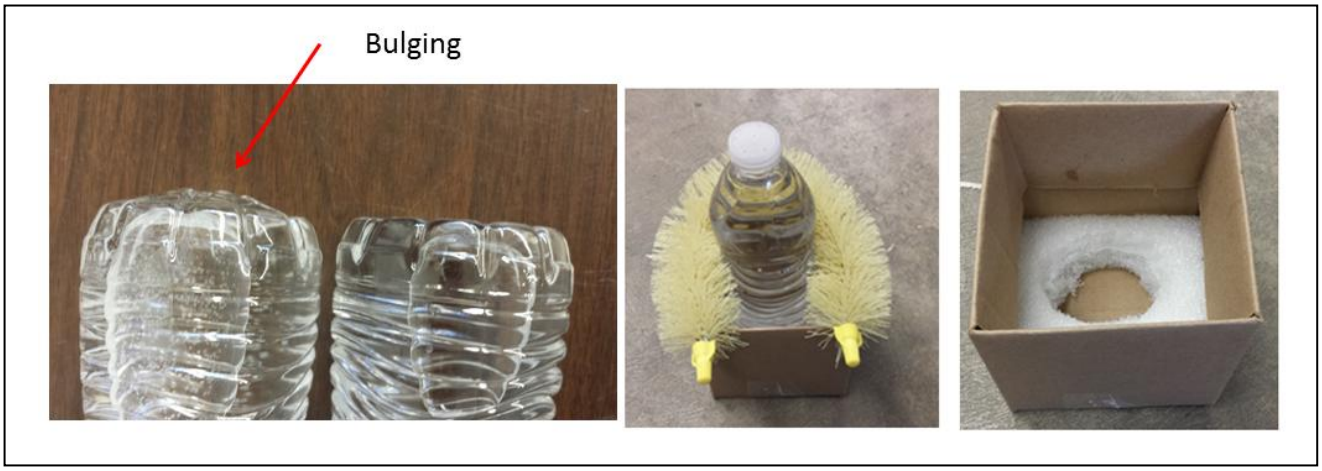

Figure 4: *Supporting Fixture to Hold Bottle Vertically During Compression Test*

Table 1: *Compression Test Data for 10 Fl. Oz. Bottles*

Sample	Temperature ($^{\circ}F$)	Maximum Load (lb)
1	123.8	38
2	119.2	58
3	118.0	48
4	112.2	46
5	111.4	59
6	110.1	30
7	109.8	57
8	105.8	57
9	104.0	55
10	66.4	70
11	66.4	78
12	47.2	72
13	44.7	81
14	40.9	86
15	39.2	103

Table 2: *Compression Test Data for 16.9 Fl. Oz. Bottles*

Sample	Temperature ($^{\circ}F$)	Maximum Load (lb)
1	125.2	10
2	121.6	73
3	117.7	13
4	116.5	24
5	115.4	61
6	112.7	63
7	112.5	59
8	111.3	59
9	108.9	76
10	102.9	63
11	64.0	45
12	63.4	60
13	62.3	73
14	51.2	83
15	51.2	76
16	51.2	72
17	40.0	67
18	39.9	47
19	37.0	70
20	32.0	72
21	31.5	84

2.4. Bulging Experiment

Bulging (extrusion at the bottom of bottle) was observed after 16.9 Fl. Oz. bottles dwelled in the chamber at $150^{\circ}F$ for three hours. Thus, an experiment was set to measure the elongation of the bottle. A dial gage with 0.001 inch accuracy was used to measure the elongation. A webcam was used so elongation could be read without having to open the chamber. Another similar bottle was also used to monitor the temperature using thermocouples. The setup is shown in Figure 5. The expansion of the wooden base was negligible, thus it was ignored. Bulging data was summarized in Table 3.

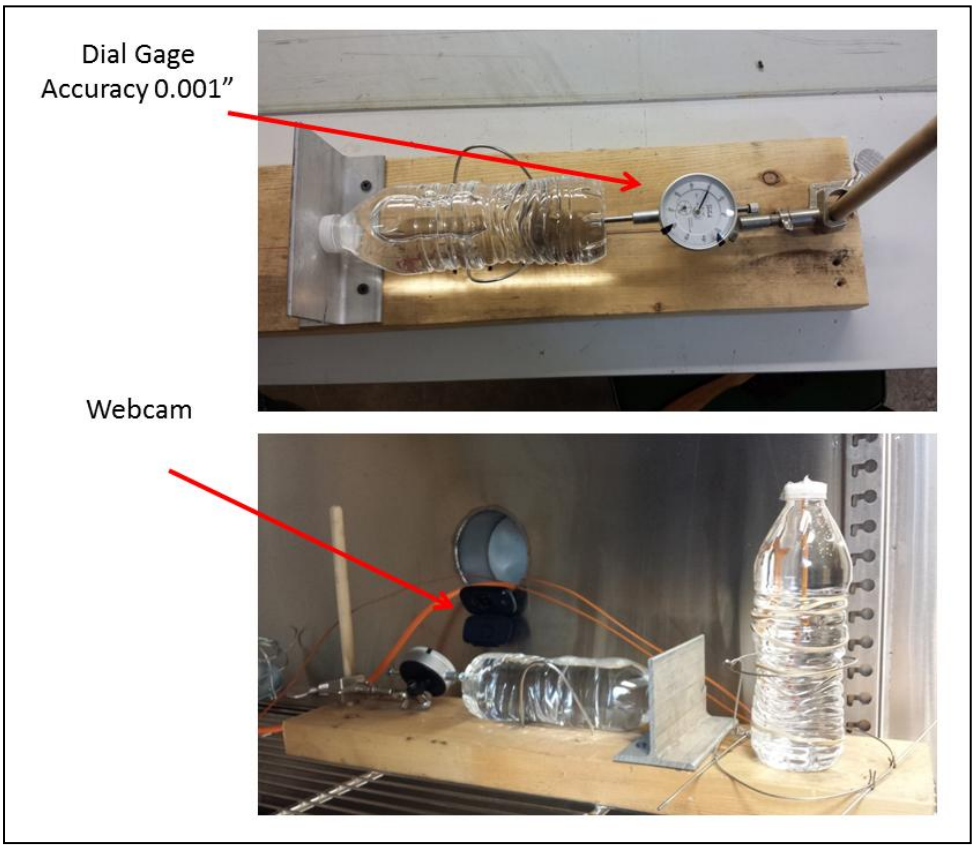

Figure 5: *Bulging Experiment Setup*

Table 3: *Bulging Data of 16.9 Fl. Oz. Bottle*

Day	Time (min)	Elongation (in)	Chamber RH (%)	Set Temperature ($^{\circ}F$)
1	0	0	6	150
1	9	0.026	6	150
1	19	0.053	6	150
1	29	0.081	6	150
1	39	0.110	6	150
1	49	0.151	6	150
1	59	0.200	6	150
1	69	0.270	6	150
1	79	0.378	6	150
1	89	0.425	6	150
1	99	0.445	6	150
1	109	0.461	6	150
1	129	0.482	6	150
1	159	0.496	6	150
1	189	0.510	6	150
1	219	0.516	6	150
1	249	0.520	6	150
1	279	0.523	6	150

1	309	0.525	6	150
2	1198	0.533	6	150
2	1208	0.535	6	150
2	1295	0.536	6	170
2	1308	0.543	6	170
2	1318	0.549	6	170
2	1328	0.554	7	170
2	1338	0.553	7	170
2	1358	0.548	7	170
2	1368	0.550	7	170
2	1378	0.550	12.4	170
2	1388	0.538	12.7	170
2	1398	0.526	13.1	170
2	1408	0.514	13.6	170

3. Results and Discussion

3.1. Effect of Temperature to Bottle Compression Strength

Data from Tables 1 and 2 were plotted in Figures 6 and 7. Even though a fixture was introduced to stabilize the 16.9 Fl. Oz. bottles during the test from the bulging, the data obtained was not as consistent as those from 10 Fl. Oz. bottles, i.e. R^2 of 0.2592 versus 0.7756. However, the trends of both bottle sizes were the same. As temperature increased, the compression strength decreased at the rate of 0.30 lb/$^\circ F$ and 0.52 lb/$^\circ F$ for 16.9 Fl. Oz. and 10 Fl. Oz. bottles, respectively.

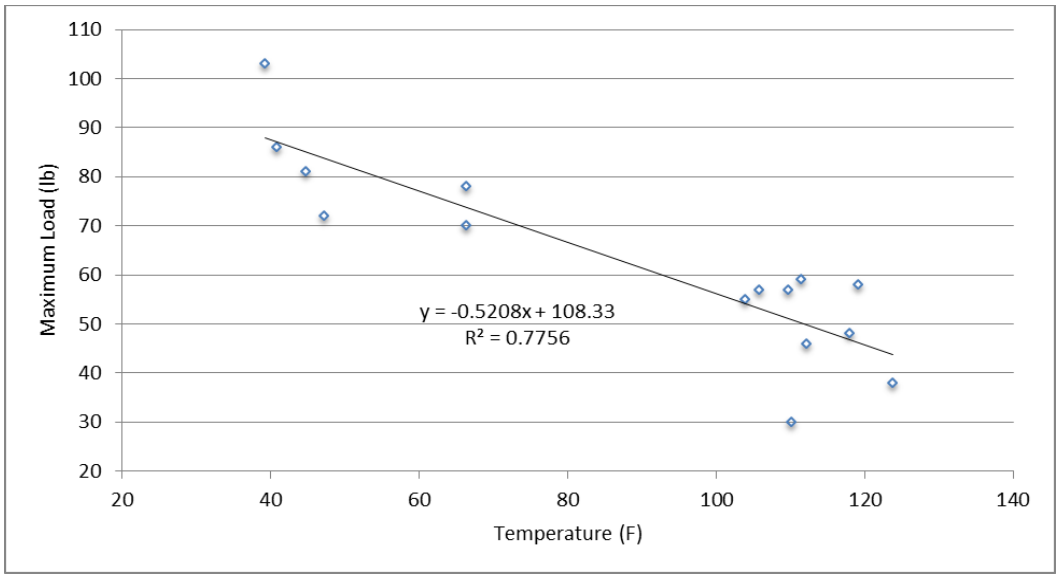

Figure 6: *Compression Strength vs Temperature for 10 Fl. Oz. Bottles*

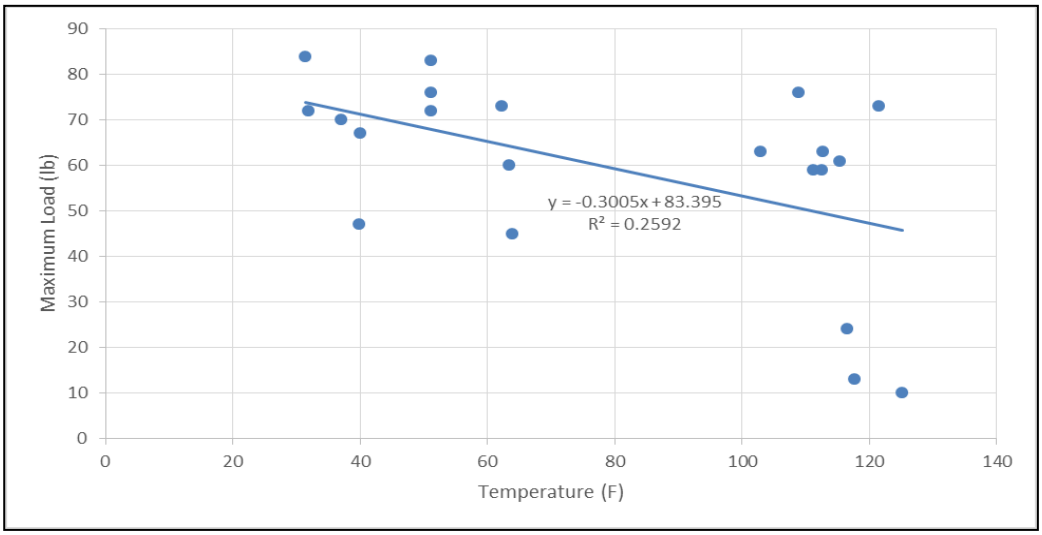

Figure 7: *Compression Strength vs Temperature for 16.9 Fl. Oz. Bottles*

3.2. Bulging

Data from Table 3 was plotted in Figure 8. The elongation was superimposed with the temperature data in Figure 9. Under $150^{\circ}F$ the bulging stopped at around 0.55 inch. However, when the chamber temperature was increased to $170^{\circ}F$, leak occurred at 1378 minutes. During the data collection, indicators of leak were an increase in chamber relative humidity from 7% to 12.4% and a drop in elongation afterward due to the release of internal pressure. Leaks were later observed at the end of the experiment, as shown in Figure 10.

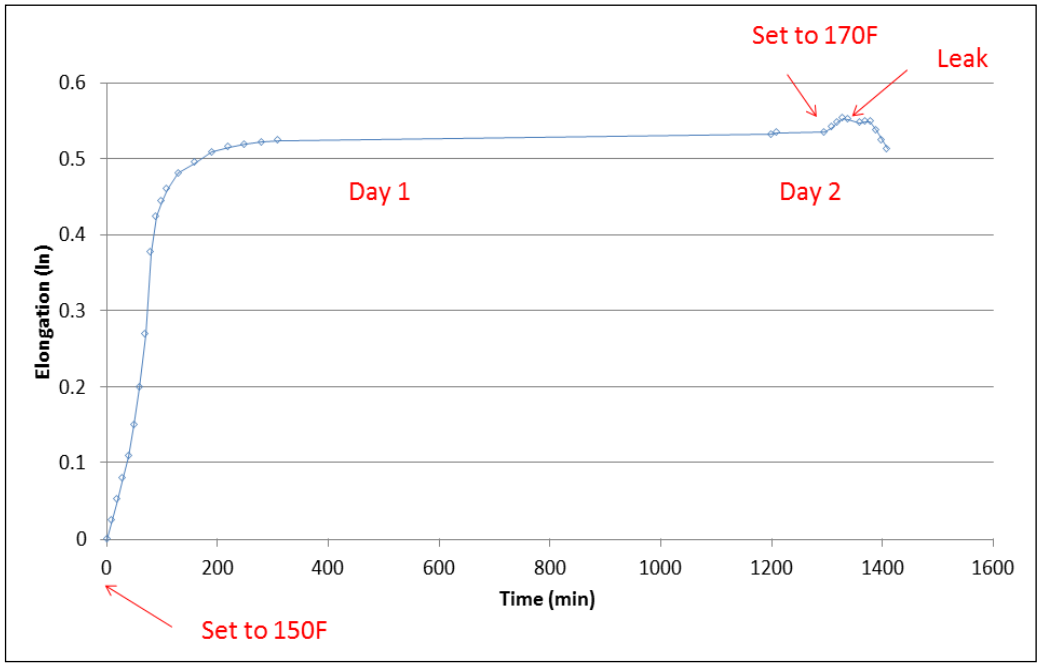

Figure 8: *Bulging Elongation with Time*

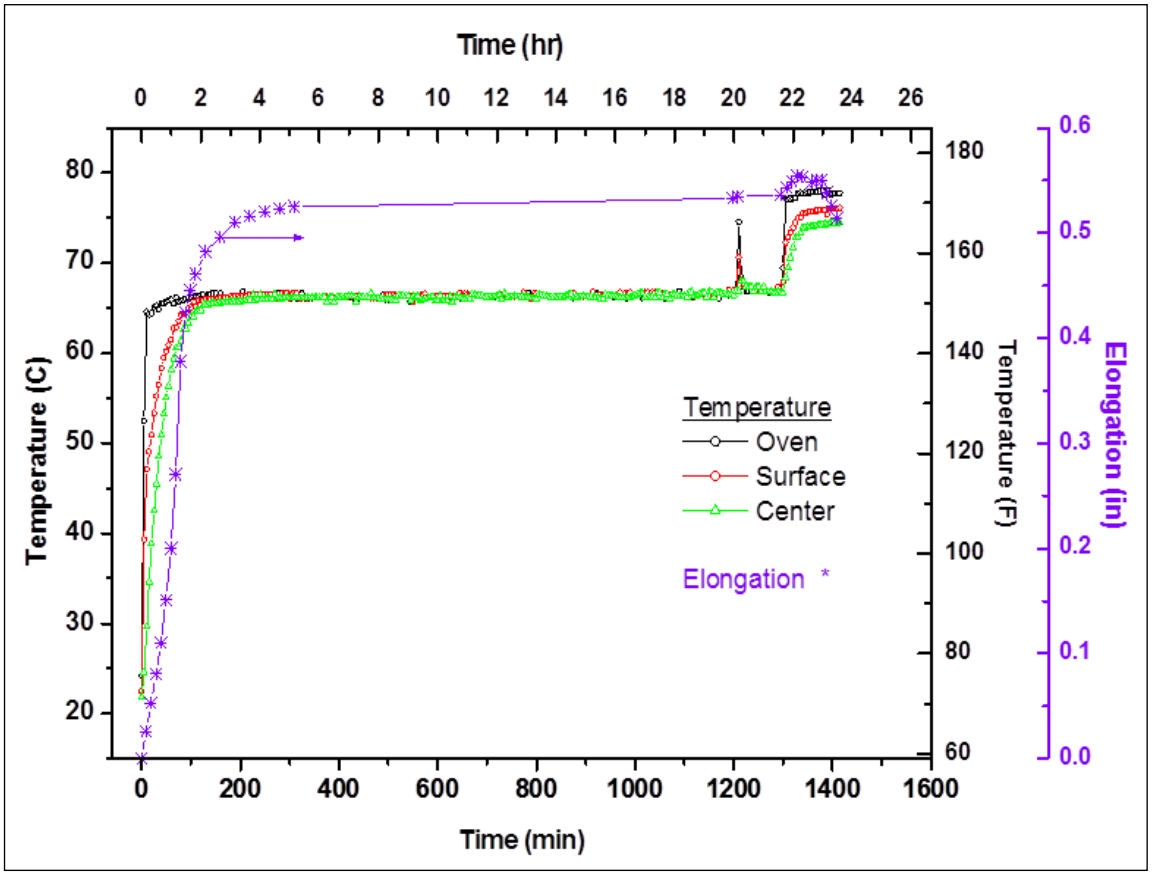

Figure 9: *Elongation with Temperature Information*

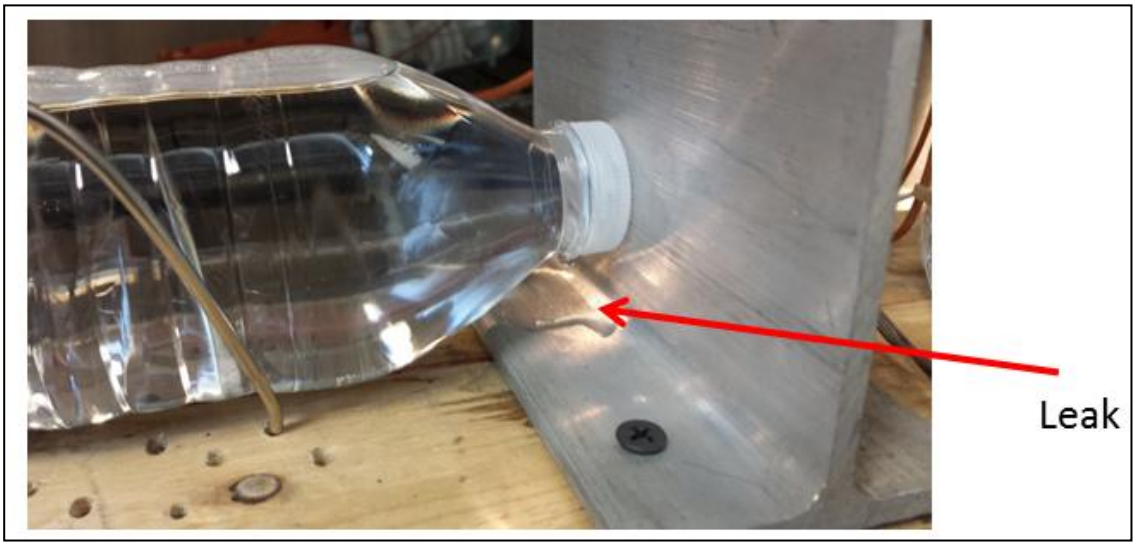

Figure 10: *Leak at Cap*

3.3. Effect of Multi-Bottle Pack

Bulging affects the stability of single bottles. However, multi-bottle packs are used during distribution. The stability of these multi-bottle packs improves significantly. It is more complex to study the effect of temperature on a multi-bottle pack. The temperature of the bottles on the pack exterior will be

different from those in the pack interior. Thus, in this study 24-bottle packs of 16.9 Fl. Oz. bottles were used. An average maximum load of ten single bottles was found to be 40.20 lb, while an average maximum load of five 24-bottle packs was found to be 1,211.33 lb or 50.47 lb/bottle. Thus, the 24-bottle pack capacity per bottle was 25.55% more than single-bottle capacity. A bottle provides lateral support to its adjacent bottles. In addition, the plastic wrap that holds the bottles together increases the pack's load bearing capacity.

4. Conclusion

The compression strength of water bottles reduces as temperature increases. Different bottle design and chemical constituents of material used will affect the strength reduction and bulging rates. However, the same trends are expected. As the bottled water industry is moving toward sustainability with thinner, thus weaker bottles, the effect from high temperature becomes more pronounced. The chamber temperatures of $150^{\circ}F$ and $170^{\circ}F$ used in this study are not uncommon in distribution environments. The three-hour chamber dwell time is also not uncommon in truck containers on a hot summer afternoon. Bulging at the bottom affects the functionality of bottles. It should also be noted that the bulging remains after the bottles cool down. Thus, a creative design is needed to reduce the bulging effect.

Acknowledgement

Part of the data was presented at the 2015 HPC Spring Meeting (April 2015). Use with permission from Christian Brothers University.

References

[1] Wikipedia, 2015: *Bottled Water in the United States*. http://en.wikipedia.org/wiki/Bottled_water_in_the_United_States

[2] Malasri, S., Pourhashemi, A., Brown, R., Harvey, M., Moats, R., Godwin, K., Aung, P., & Laney, J. *Effect of Temperature on Static and Impact Properties of New Softwood Pallets*. International Journal of Advanced Packaging Technology. 2013. 1 (1) 30-39.

[3] Selke, S., 1997: *Understanding Plastics Packaging Technology*. Hanser/Garner Publications. 28-30.

[4] Sastri, V.R., 2014: *Plastics in Medical Devices*. Elsevier. 150-160.

[5] Wikipedia, 2015: *Polyethylene Terephthalate*. http://en.wikipedia.org/wiki/Polyethylene_terephthalate

[6] McCabe, W., Smith, J., and Harriott, P., 2004. *Unit Operations of Chemical Engineering*. McGraw Hill. 311.

Cloud Publications
International Journal of Advanced Packaging Technology
2015, Volume 3, Issue 1, pp 158-168, Article ID Tech-485
ISSN 2349-6665, doi 10.23953/cloud.ijapt.20

Research Article **Open Access**

Insulation Effectiveness of Rice Hull

Siripong Malasri[1], Poomtawan Tiapradit[2], Stephen Russell[1], Possawat Poonpurmsiri[2], Chonnavee Tarkarnviroj[2], Ali Pourhashemi[1], Robert Moats[1] and Bradley Hudson[1]

[1]Healthcare Packaging Consortium, Christian Brothers University, 650 East Parkway South, Memphis, TN, USA
[2]Department of Packaging and Materials Technology, Kasetsart University, 50 Ngam Wong Wan Road, Lad Yao, Chatuchak, Bangkok 10900, Thailand

Correspondence should be addressed to Siripong Malasri, pong@cbu.edu

Publication Date: 28 September 2015

DOI: https://doi.org/10.23953/cloud.ijapt.20

Editor-in-Chief: **Dr. Siripong Malasri**, Christian Brothers University, Memphis, TN, USA

Abstract A previous study showed loose rice hull had reasonable shock absorption even though it was not as effective as bubble wrap and anti-vibration pad. Another study showed rice hull's shock absorption was better than larger grain size crumb rubber, but worse than finer grain size crumb rubber and coconut fiber. A comparative study showed that rice hull was more effective as an insulation material than coconut fiber sheet but less effective than crumb rubber. In this study, a new insulated container was envisioned. Its wall consisted of two layers of single-wall corrugated boards with rice hull filled in the gap between them. Temperature data was collected for three thickness of rice hull, i.e., 0.5", 1.0", and 1.5". For each thickness, nine combinations of three outside temperatures (90°F, 120°F, and 150°F) and three starting interior temperatures (35°F, 45°F, and 55°F) were used. A neural network was trained to recognize the patterns of the interior temperature changes over time. The trained network can then be used for any combinations of exterior and starting interior temperatures. It assists packaging professionals in determining a proper thickness of rich hull needed for distribution. Rice hull insulated containers are suitable for a short distribution route.

Keywords *Rice Hull; Insulated Container; Heat Transfer; Artificial Neural Network; Sustainability*

1. Introduction

Loose rice hull reduced impact acceleration significantly but was less effective than bubble wrap, anti-vibration pad, coconut fiber and fine grain crumb rubber [1, 2]. However, rice hull and coconut fiber are agricultural waste products, which are environmental friendly. A comparative study [3] was

performed to see the insulation effectiveness of rice hull, coconut fiber, and crumb rubber. They are potential insulation materials of future environmentally friendly insulated containers. Rice hull is more effective than coconut fiber sheet but less effective than crumb rubber.

In this study rice hull was put in a gap between two corrugated boards with three different gap widths. A total of nine combinations of exterior and interior temperatures were included in the study. Interior temperature versus time data was recorded. A neural network was trained to recognize the interior temperature changes with time under different exterior and interior temperature settings and different gap widths. The purpose of this study is to develop a neural network that can predict the time required to bring the interior temperature to a specified level for a given set of exterior and interior temperature combinations and rice hull thickness.

2. Materials and Methods

An insulated container was built from two single-wall corrugated boxes; 7”x7”x7” for the outer box and 4”x4”x4” for the inner box as shown in Figure 1. The inner box was sealed with two layers of 0.5-inch insulating sheathing on five sides (3 sides, bottom, and top). One side was spaced from the outer box which created a gap to be filled with rice hull. Three different gap widths were used in the study; 0.5”, 1.0”, and 1.5”.

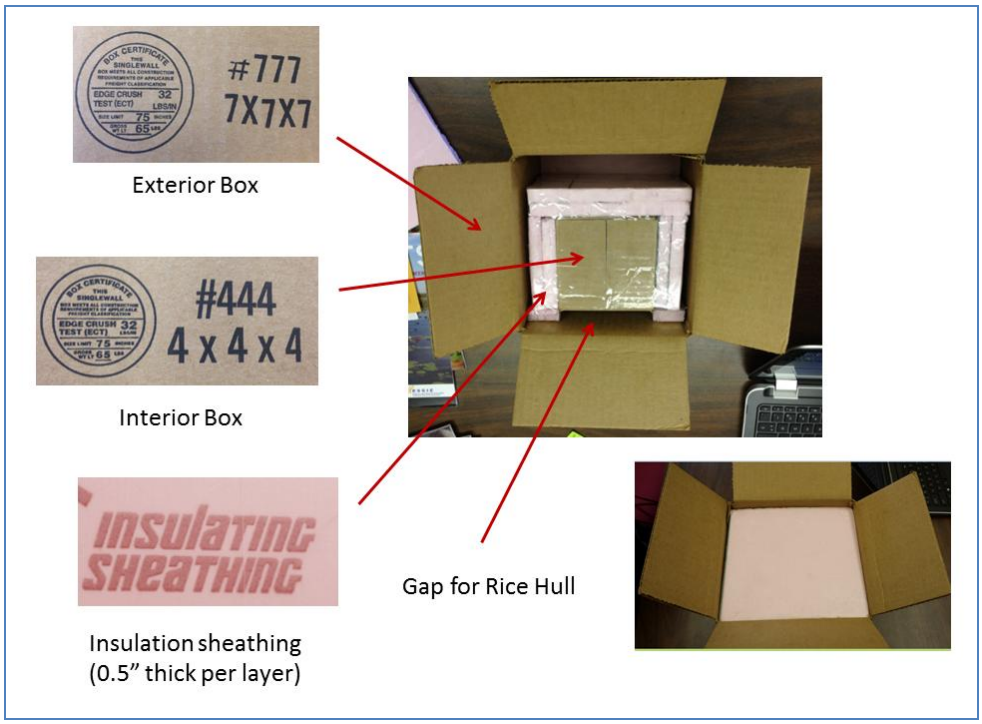

Figure 1: *Insulated Container with Sealed Inner Box for One-Direction Heat Flow*

A thermocouple was inserted inside the inner box. The box was sealed and placed in an altitude chamber. The thermocouple was connected to a data acquisition system as shown in Figure 2. It should be noted that the four insulated containers in the chamber shown in Figure 2 were taken from the previous comparative study [3] on insulation effectiveness of rice hull, coconut fiber, crumb rubber, and air.

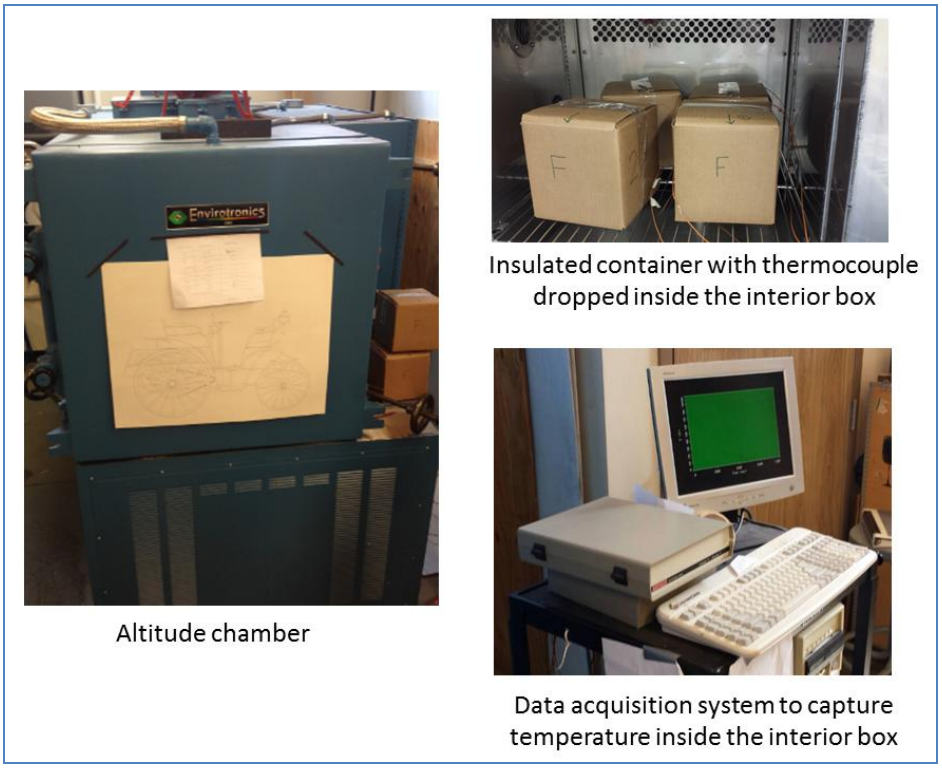

Figure 2: *Insulated Container, Altitude Chamber, Thermocouple, and Data Acquisition System*

The insulated container was first cooled down to a specified low temperature to simulate a cool container. Then it was raised to a specified high temperature to simulate a hot outside environment such as in a warehouse or inside a truck. A total of nine combinations as shown in Table 1 were performed for each gap thickness, i.e., 0.5”, 1.0”, or 1.5”.

Table 1: *Interior and Exterior Temperature Combinations for Each Gap Thickness*

		Interior Temperature		
		35°F	45°F	55°F
Exterior Temperature	90°F	35°F - 90°F	45°F - 90°F	55°F - 90°F
	120°F	35°F - 120°F	45°F - 120°F	55°F - 120°F
	150°F	35°F - 150°F	45°F - 150°F	55°F - 150°F

NeuroShell2 [4] was used to train a neural network to recognize temperature changes with time under each temperature combination and gap thickness.

3. Results and Discussion

Collected temperature data were plotted in Figures 3 – 5 for different thicknesses and temperature combinations.

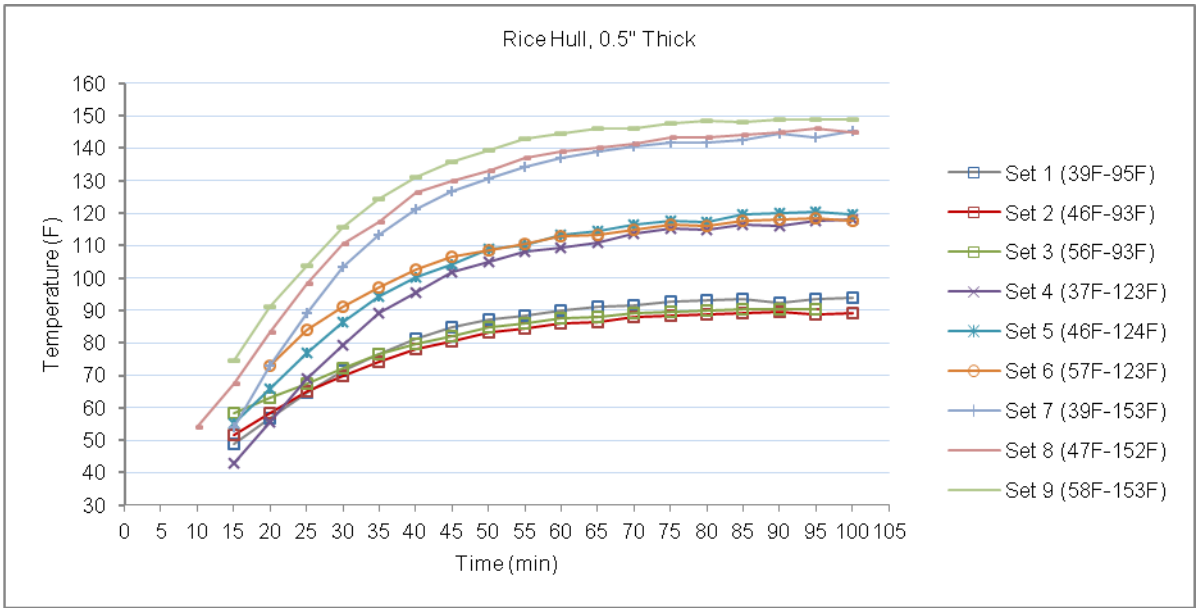

Figure 3: *Temperature Data for 0.5" Thick Rick Hull*

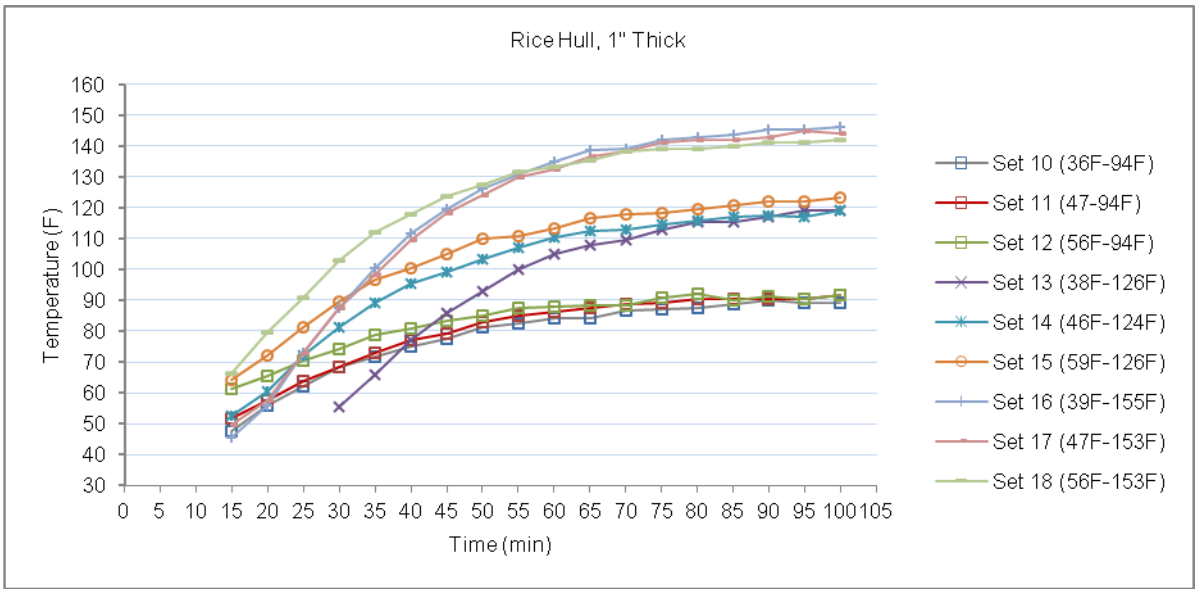

Figure 4: *Temperature Data for 1.0" Thick Rick Hull*

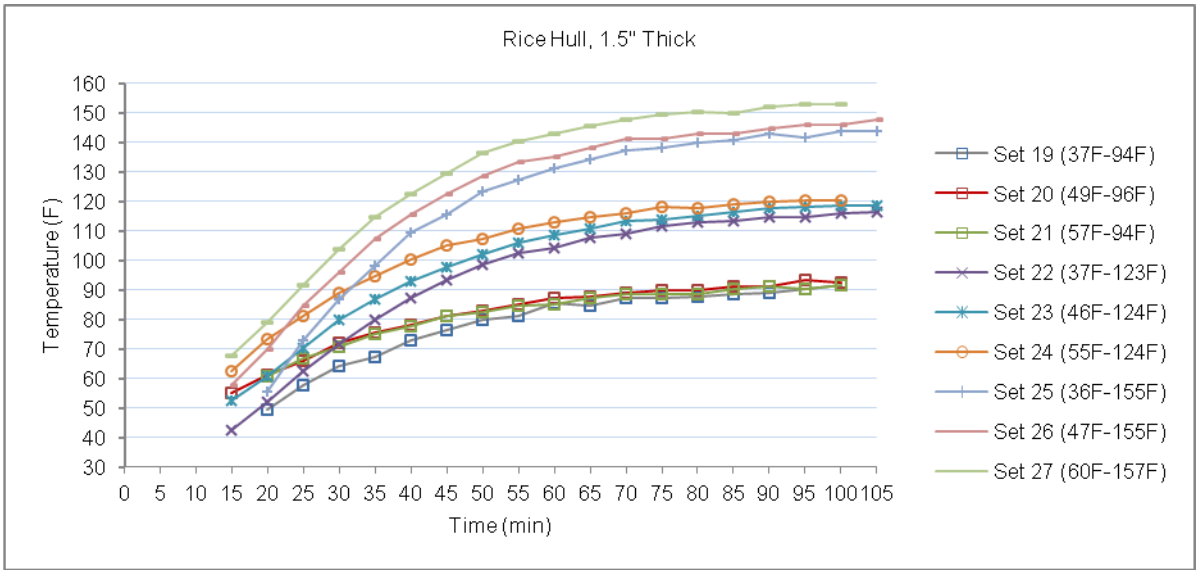

Figure 5: *Temperature Data for 1.5" Thick Rick Hull*

Collected data were tabulated for the neural network training and validation. Table 2 shows sample data obtained from the Set 2 temperature combination, which is one of the 27 sets. Inputs to the neural network are thickness of rice hull (Thick), exterior temperature (Chamber), starting temperature inside the inner box (Inner), the current temperature (Temp), and the time at current temperature (Time). The "T" and "V" marks indicate that the record is used for "Training" or "Validating."

Table 2: *Neural Network Data from Set 2 Temperature Combination*

	Input	Input	Input	Input	Output	
	(in)	(°F)	(°F)	(°F)	(min)	
Set	Thick	Chamber	Inner	Temp	Time	Mark
2	0.5	93	46	51.5	15	T
2	0.5	93	46	58.4	20	T
2	0.5	93	46	65.1	25	T
2	0.5	93	46	69.7	30	T
2	0.5	93	46	74.2	35	T
2	0.5	93	46	77.9	40	T
2	0.5	93	46	80.5	45	T
2	0.5	93	46	83.1	50	T
2	0.5	93	46	84.5	55	T
2	0.5	93	46	85.9	60	T
2	0.5	93	46	86.3	65	T
2	0.5	93	46	87.9	70	T
2	0.5	93	46	88.4	75	T
2	0.5	93	46	88.8	80	T
2	0.5	93	46	89.3	85	T
2	0.5	93	46	89.7	90	T
2	0.5	93	46	88.9	95	T
2	0.5	93	46	89.2	100	T
2	0.5	93	46	71.8	32	V
2	0.5	93	46	84.3	53	V
2	0.5	93	46	89.2	84	V

The network performance was evaluated and summarized in Table 3. “Seen Cases” are those used in network training, while “Unseen Cases” are those used in validating the network. “All Cases” are the sum of seen and unseen cases. In all categories, approximately 97% of each case gave an output within 10% error.

Table 3: *Neural Network Performance*

Category	Number Of Cases	<=5% Error	>5% to 10% Error	>10% to 20% Error	>20% Error
All Cases	568	460 (80.99%)	92 (16.20%)	14 (2.46%)	2 (0.35%)
Seen Cases	487	387 (79.47%)	86 (17.66%)	14 (2.87%)	0 (0%)
Unseen Cases	81	73 (90.12%)	6 (7.41%)	0 (0%)	2 (2.47%)

Once validated, a network source code was obtained from NeuroShell 2 as shown in Appendix. A spreadsheet was developed as a stand-alone application so the user does not need to have the NeuroShell 2 software. Figure 6 shows the input and output of the rice hull spreadsheet. The thickness used was 0.75 inch which is not part of the study. However, the neural network interpolated the result as 23.4 minutes, which is between 16.5 minutes for 0.5” thickness and 24.2 minutes for 1.0” thickness.

	A	B
1	input	
2	Insulation Thickness (in)	0.75
3	Expected Chamber Temperature (°F)	150
4	Content Starting Temperature (°F)	40
5	Content Critical Temperature (°F)	60
6		
7		
8	Output	
9	Maximum Travel Time (min)	23.4
10		

Figure 6: *Rice Hull Spreadsheet*

Figure 7 shows a comparison of different thicknesses of rice hull. As expected when the thickness was increased from 0.5” to 1.0”, it took a longer time for the heat to penetrate into the inner box. However, when the thickness was increased from 1.0” to 1.5”, the times were comparable at higher temperatures. The validity of 1.5” experiment is questionable. Thus, the use of this neural network should be limited to 1.0” thickness or less.

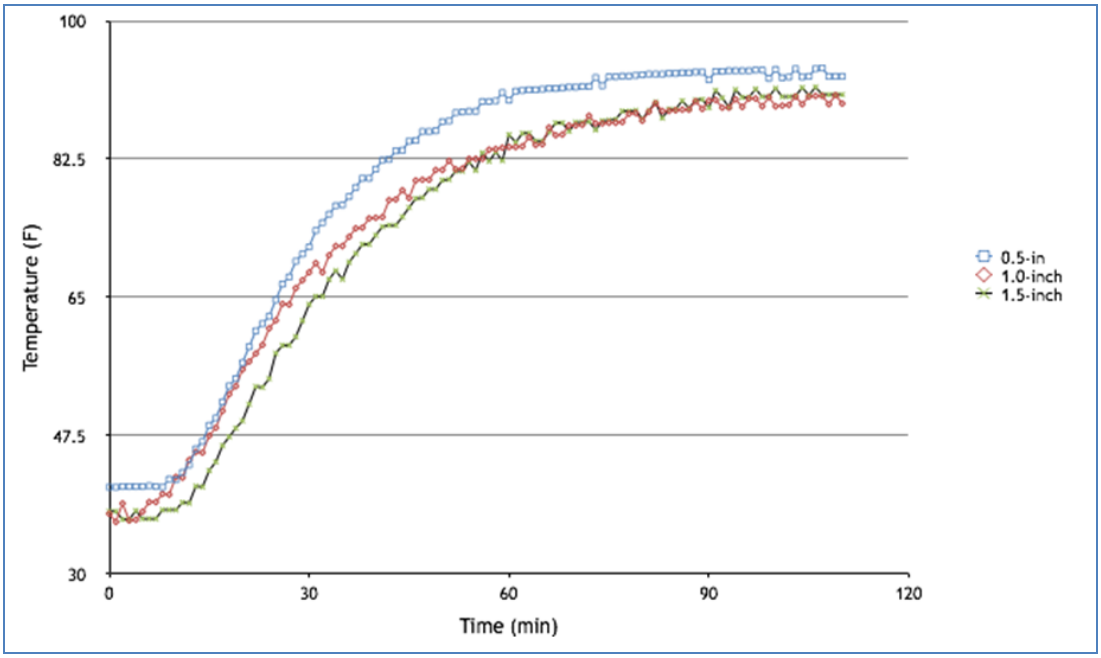

Figure 7: *Comparison of Different Rice Hull Thickness at a Comparable Temperature Range*

4. Conclusion

As seen from Figures 3 – 5, the interior temperature rises to exterior temperature in less than 1.5 hours. Depending on the threshold of the interior temperature, i.e., the temperature limit that will not affect the content, the time duration is even less. Thus, rice hull insulated containers are not suitable for a longer distribution route. It is suitable for distribution within a city, such as a distribution of medical related items.

The neural network performance is excellent. To determine an appropriate rice hull thickness, a thickness is entered into the spreadsheet along with the exterior, starting interior, and the critical or threshold temperatures. The network then gives an output of time before that the interior temperature rises to the critical temperature. It is possible to manufacture insulated containers with different thicknesses for different ranges of temperature combinations.

References

[1] Malasri, S., Stevens, R., Othmani, A., Harvey, M., Griffith, I., Guerrero, D., Johnson, M., Kist, M., Nguyen, C., Polania, S., Qureshi, A. and Sanchez-Luna, Y. *Rice Hulls as a Cushioning Materials*. International Journal of Advanced Packaging Technology. 2014. 2 (1) 112-118.

[2] Alnashwan, W., Aloumi, B., Malasri, S., Kist, M., Othmani, A., Fotso, R., Johnson, M., Polania, S. and Sanchez-Luna, Y. *Shock Absorption of Crumb Rubber and Coconut Fiber.* International Journal of Advanced Packaging Technology. 2014. 2(1) 119-128.

[3] Russell, S., Malasri, S., Poonpurmsiri, P., Tarkarnviroj, C., Tiapradit, P., Pourhashemi, A., Moats, R. and Hudson, B. *Insulation Effectiveness Comparison of Rice Hull, Coconut Fiber, and Crumb Rubber.* Proceedings of the PACKCON 2015 Conference. 2015. 4-7.

[4] Ward Systems Group, Inc. *NeuroShell 2.* http://www.wardsystems.com/neuroshell2.asp (As of September 7, 2015)

Appendix

Generic source code generated by NeuroShell 2:

```
netsum
feature2(25)
Note - the following are names of inputs and outputs:
Note - inp(1) is Thick
Note - inp(2) is Chamber
Note - inp(3) is Inner
Note - inp(4) is Temp
Note - outp(1) is Time
if (inp(1)<0.5) then inp(1) = 0.5
if (inp(1)>1.5) then inp(1) = 1.5
inp(1) = (inp(1) - 0.5)
if (inp(2)<93) then inp(2) = 93
if (inp(2)>157) then inp(2) = 157
inp(2) = (inp(2) - 93) /64
if (inp(3)<36) then inp(3) = 36
if (inp(3)>60) then inp(3) = 60
inp(3) = (inp(3) - 36) /24
if (inp(4)<42.5) then inp(4) = 42.5
if (inp(4)>153) then inp(4) = 153
inp(4) = (inp(4) - 42.5) /110.5
netsum = -77.42249
netsum = netsum + inp(1) * 1.829195
netsum = netsum + inp(2) * 51.18296
netsum = netsum + inp(3) * 2.897887
netsum = netsum + inp(4) * 25.01999
feature2(1) = 1 / (1 + exp(-netsum))
netsum = -34.30855
netsum = netsum + inp(1) * 3.381074
netsum = netsum + inp(2) * 0.6520041
netsum = netsum + inp(3) * 5.827303
netsum = netsum + inp(4) * 28.46277
feature2(2) = 1 / (1 + exp(-netsum))
netsum = 11.80751
netsum = netsum + inp(1) * -0.7572004
netsum = netsum + inp(2) * 16.44867
netsum = netsum + inp(3) * 1.609694
netsum = netsum + inp(4) * -30.24881
feature2(3) = 1 / (1 + exp(-netsum))
netsum = -19.74744
netsum = netsum + inp(1) * 11.08275
netsum = netsum + inp(2) * -11.2922
netsum = netsum + inp(3) * -11.15322
netsum = netsum + inp(4) * 18.53922
feature2(4) = 1 / (1 + exp(-netsum))
netsum = -22.27897
netsum = netsum + inp(1) * 7.165064
netsum = netsum + inp(2) * -16.6314
netsum = netsum + inp(3) * -5.059668
netsum = netsum + inp(4) * 32.52828
feature2(5) = 1 / (1 + exp(-netsum))
netsum = 0.5769625
netsum = netsum + inp(1) * 3.890337
netsum = netsum + inp(2) * -3.766037
netsum = netsum + inp(3) * 1.540869
netsum = netsum + inp(4) * -21.33095
feature2(6) = 1 / (1 + exp(-netsum))
netsum = -2.477142
netsum = netsum + inp(1) * -0.6397823
netsum = netsum + inp(2) * 0.6325201
netsum = netsum + inp(3) * 0.3864034
```

```
netsum = netsum + inp(4) * -1.387421
feature2(7) = 1 / (1 + exp(-netsum))
netsum = 2.504263E-02
netsum = netsum + inp(1) * 4.917343
netsum = netsum + inp(2) * -5.351194
netsum = netsum + inp(3) * 1.058412
netsum = netsum + inp(4) * -3.155575
feature2(8) = 1 / (1 + exp(-netsum))
netsum = -6.079099
netsum = netsum + inp(1) * -18.85942
netsum = netsum + inp(2) * -29.57689
netsum = netsum + inp(3) * -22.49723
netsum = netsum + inp(4) * 23.33121
feature2(9) = 1 / (1 + exp(-netsum))
netsum = -2.30052
netsum = netsum + inp(1) * -0.7811611
netsum = netsum + inp(2) * 0.8631783
netsum = netsum + inp(3) * 0.5986145
netsum = netsum + inp(4) * -1.770426
feature2(10) = 1 / (1 + exp(-netsum))
netsum = -1.613661
netsum = netsum + inp(1) * 1.117724
netsum = netsum + inp(2) * 1.136369
netsum = netsum + inp(3) * -1.109539
netsum = netsum + inp(4) * -0.7703084
feature2(11) = 1 / (1 + exp(-netsum))
netsum = -35.36966
netsum = netsum + inp(1) * 0.5096668
netsum = netsum + inp(2) * -37.69466
netsum = netsum + inp(3) * -4.542458
netsum = netsum + inp(4) * 78.2354
feature2(12) = 1 / (1 + exp(-netsum))
netsum = -17.01482
netsum = netsum + inp(1) * -3.632286
netsum = netsum + inp(2) * -16.90736
netsum = netsum + inp(3) * 7.179433
netsum = netsum + inp(4) * 23.45917
feature2(13) = 1 / (1 + exp(-netsum))
netsum = -2.351869
netsum = netsum + inp(1) * -0.7066271
netsum = netsum + inp(2) * 0.7919896
netsum = netsum + inp(3) * 0.516634
netsum = netsum + inp(4) * -1.666512
feature2(14) = 1 / (1 + exp(-netsum))
netsum = 0.4725413
netsum = netsum + inp(1) * -6.267524
netsum = netsum + inp(2) * -14.388
netsum = netsum + inp(3) * -21.67318
netsum = netsum + inp(4) * -3.762873
feature2(15) = 1 / (1 + exp(-netsum))
netsum = -9.839572
netsum = netsum + inp(1) * 5.391343
netsum = netsum + inp(2) * 9.922738
netsum = netsum + inp(3) * -7.104128
netsum = netsum + inp(4) * -0.6108747
feature2(16) = 1 / (1 + exp(-netsum))
netsum = -32.93026
netsum = netsum + inp(1) * 1.181343
netsum = netsum + inp(2) * -47.83091
netsum = netsum + inp(3) * -1.249812
netsum = netsum + inp(4) * 78.79494
feature2(17) = 1 / (1 + exp(-netsum))
netsum = -2.00805
netsum = netsum + inp(1) * -1.036443
netsum = netsum + inp(2) * 0.7159287
```

```
netsum = netsum + inp(3) * 0.7049346
netsum = netsum + inp(4) * -1.656927
feature2(18) = 1 / (1 + exp(-netsum))
netsum = -3.143473
netsum = netsum + inp(1) * -9.047296
netsum = netsum + inp(2) * 1.569484
netsum = netsum + inp(3) * -5.540841
netsum = netsum + inp(4) * -1.248824
feature2(19) = 1 / (1 + exp(-netsum))
netsum = -7.864933
netsum = netsum + inp(1) * -9.619619
netsum = netsum + inp(2) * 2.728712
netsum = netsum + inp(3) * 9.075184
netsum = netsum + inp(4) * -5.947243
feature2(20) = 1 / (1 + exp(-netsum))
netsum = -26.06628
netsum = netsum + inp(1) * -5.060097
netsum = netsum + inp(2) * -32.91682
netsum = netsum + inp(3) * 14.04668
netsum = netsum + inp(4) * 34.43976
feature2(21) = 1 / (1 + exp(-netsum))
netsum = 3.527127
netsum = netsum + inp(1) * -1.052538
netsum = netsum + inp(2) * 5.13706
netsum = netsum + inp(3) * 3.000223E-02
netsum = netsum + inp(4) * -9.525806
feature2(22) = 1 / (1 + exp(-netsum))
netsum = 3.17608
netsum = netsum + inp(1) * -2.799266
netsum = netsum + inp(2) * -4.537488
netsum = netsum + inp(3) * 5.004307
netsum = netsum + inp(4) * 1.735753
feature2(23) = 1 / (1 + exp(-netsum))
netsum = -1.901363
netsum = netsum + inp(1) * -1.14969
netsum = netsum + inp(2) * 0.4750226
netsum = netsum + inp(3) * 0.7146776
netsum = netsum + inp(4) * -1.402273
feature2(24) = 1 / (1 + exp(-netsum))
netsum = -37.89122
netsum = netsum + inp(1) * -17.27869
netsum = netsum + inp(2) * -1.996307
netsum = netsum + inp(3) * 10.17964
netsum = netsum + inp(4) * 32.27686
feature2(25) = 1 / (1 + exp(-netsum))
netsum = 3.233013
netsum = netsum + feature2(1) * -6.513914
netsum = netsum + feature2(2) * 5.922116
netsum = netsum + feature2(3) * -0.8871983
netsum = netsum + feature2(4) * -4.821428
netsum = netsum + feature2(5) * 3.682183
netsum = netsum + feature2(6) * -0.4269779
netsum = netsum + feature2(7) * -2.162769
netsum = netsum + feature2(8) * -0.6949077
netsum = netsum + feature2(9) * -1.166742
netsum = netsum + feature2(10) * -2.15929
netsum = netsum + feature2(11) * -1.563802
netsum = netsum + feature2(12) * 0.7780318
netsum = netsum + feature2(13) * 11.13845
netsum = netsum + feature2(14) * -2.118476
netsum = netsum + feature2(15) * -3.005923
netsum = netsum + feature2(16) * -0.7979156
netsum = netsum + feature2(17) * 0.9646804
netsum = netsum + feature2(18) * -2.262065
netsum = netsum + feature2(19) * -2.731027
```

```
netsum = netsum + feature2(20) * 0.479648
netsum = netsum + feature2(21) * -4.598935
netsum = netsum + feature2(22) * -1.077305
netsum = netsum + feature2(23) * -1.168869
netsum = netsum + feature2(24) * -2.387797
netsum = netsum + feature2(25) * -2.281764
outp(1) = 1 / (1 + exp(-netsum))
outp(1) = 105 *  (outp(1) - .1) / .8  + 10
```

HEALTHCARE PACKAGING CONSORTIUM

Cloud Publications
The Open Access Publisher

Date: December 28, 2015

Siripong Malasri, **PhD, PE, CPLP Professional**
Editor-in-Chief, International Journal of Advanced Packaging Technology (ISSN 2349-6665)
Director, Healthcare Packaging Consortium, Christian Brothers University, 650 East Parkway South, Memphis, TN 38104, USA. Phone 1-901-321-3419; Fax 1-901-321-3402; Email pong@cloud-journals.com

Dear Readers:

We have reached the end of Volume 3 of the **International Journal of Advanced Packaging Technology**. On behalf of the journal, I would like to thank the authors for their articles. I would also like to thank the Volume 3 editors, reviewers, and technical assistant:

- M.S.R. Airan, PhD, Cloud Publications, India
- Amit Chauhan, Cloud Publications, India
- Kyle Dunno, PhD, CPLP Professional, Sealed Air, USA
- Stephen Russell, Christian Brothers University, USA
- Tunyarut Jinkarn, PhD, Kasetsart University, Thailand
- Eric Joneson, CPLP Professional, Lansmont, USA
- Ali Pourhashemi, PhD, Christian Brothers University, USA
- Asit Ray, PhD, Christian Brothers University, USA
- Mike Tune, CPP, Bayer Consumer Care, USA

Happy New Year 2016,

S. Malasri

Siripong Malasri